8-2000

Remediation of borosilicate Raschig rings

Kenneth Ross Givens

To the Graduate Council:

I am submitting herewith a thesis written by Kenneth Ross Givens entitled "Remediation of borosilicate Raschig rings." I have examined the final electronic copy of this thesis for form and content and recommend that it be accepted in partial fulfillment of the requirements for the degree of Master of Science, with a major in Chemical Engineering.

Jack Watson, Major Professor

We have read this thesis and recommend its acceptance:

John W. Prados, George C. Frazier
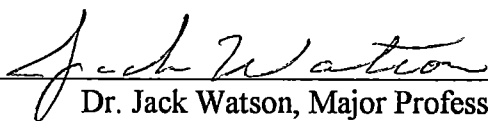
Accepted for the Council:

Carolyn R. Hodges

Vice Provost and Dean of the Graduate School

(Original signatures are on file with official student records.)
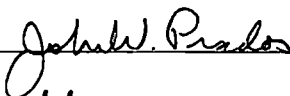
To the Graduate Council

I am submitting herewith a thesis written by Kenneth Ross Givens entitled "Remediation of Borosilicate Raschig Rings " I have examined the final copy of this dissertation for form and content and recommend that it be accepted in partial fulfillment of the requirements for the degree of Master of Science, with a major in Chemical Engineering

Dr. Jack Watson, Major Professor

We have read this thesis
and recommend its acceptance.

Accepted for the Council

Associated Vice Chancellor and
Dean of the The Graduate School

REMEDIATION OF BOROSILICATE RASCHIG RINGS

A Thesis

Presented for the

Master of Science

Degree

The University of Tennessee, Knoxville

Kenneth Ross Givens

August 2000

DEDICATION

This thesis is dedicated to my parents

Lanny and Barbara

who gave me the desire to achieve.

ACKNOWLEDGMENTS

There are many people to whom I am grateful for making my research possible   I have benefited greatly from interacting with the faculty and fellow researchers at the University of Tennessee and the Oak Ridge National Laboratory. I am particularly grateful to my Thesis Committee, Dr. Jack Watson, Dr. George Frazier, and Dr John Prados for their support

I would also like to extend special gratitude to Oak Ridge National Laboratory for the opportunity to perform the research. I would like to thank Brad Patton, whose guidance allowed me to obtain the funding to pursue my research topic, and the staff of the Radiochemical Development Facility, whose efforts made this project possible

ABSTRACT

The legacy of the nuclear arms race has left numerous environmental remediation challenges. For example, a common practice from the 1950s to the 1970s for nuclear criticality control of fissile solutions in storage tanks was the use of borosilicate Raschig rings However, this practice subsided with the uncertainty in the long-term consistency of the boron concentration in the Raschig rings The result was numerous abandoned tanks that are relatively filled with contaminated borosilicate Raschig rings

The focus of this study was on a radioactive waste stream from an uranium/thorium separation process that was conducted in the 1970s. The primary radioactive contaminants of this waste stream were thorium-228/229 and the associated decay products. Motivation for remediation of the Raschig rings is based on the associated costs of disposal of large volumes of radioactively contaminated Raschig rings. Additional inspiration behind this particular waste stream is the interest in thorium-229 as a bio-medical generator for alpha radioimmunotherapy

In this study, successful remediation of radioactively contaminated borosilicate Raschig rings was achieved using a nitric acid solvent/ultrasonic agitation method followed by ion exchange separation and a combination surfactant/ultrasonic volume reduction method. Both methods resulted in a successful remediation with greater than 99% removal of the radioactive contaminants Furthermore, successful recovery of the thorium-229 was achieved through a combination of batch anion and cation ion exchange processes Consequently, this success has allowed clinical trials to begin on a new treatment for mylegeneous leukemia using the decay products from thorium-229

TABLE OF CONTENTS

LIST OF FIGURES

LIST OF TABLES

NOMENCLATURE

A	Area
a	Empirical parameter for surface tension
A	Empirical parameter for liquid viscosity
A_s	Surface area of resin particles
b	Empirical parameter for surface tension
B	Empirical parameter for liquid viscosity
c	Sound velocity
C_A,	Concentration of species A
C_{A0}	Initial concentration of species A
C_{Asi}	Interfacial concentration of species A
C_{As}	Average concentration of species A in the solid phase
C_{Ai}	Interfacial concentration of species A in the fluid phase
C_A^*	Equilibrium concentration of species A between fluid and solid phase
C_p	Heat capacity at constant pressure
C_v	Heat capacity at constant volume
D_A	Effective diffusion
DWC	Dry weight capacity
d_p	Diameter of the particle
dx	Differential increment in the x direction
E	Energy density
E_D	Eddy diffusion coefficient
E_t	Energy of the acoustic wave
E_{Uv}	Ultrasonic eddy diffusivity
E_v	Eddy viscosity
f	Applied frequency
g_A	Gram of species A

I	Acoustic intensity
I_o	Initial acoustic intensity
k	Effective mass transfer coefficient
k_f	Film mass transfer coefficient
k_s	Solid mass transfer coefficient
K	Polytropic index for specified gas
K_d	Dissociation constant
K_f	Overall effective mass transfer coefficient
KE	Kinetic energy
$\overline{k_M}$	Mean kinematic viscosity
k_V	Kinematic viscosity
M_R	Mass of resin
N_A	Normality of species A
n_{Ax}	Molar flux of species A
P_a	Acoustic pressure
P_A	Oscillating acoustic pressure
P_B	Blake threshold pressure
P_{bub}	Bubble pressure
P'_{bub}	New bubble pressure
P_g	Gas pressure of bubble
P'_g	New gas pressure
P_h	Hydrostatic pressure of bubble
P'_h	New hydrostatic pressure
P_L	Liquid pressure of bubble
P'_L	New liquid pressure
P_v	Vapor pressure of bubble
R	New bubble radius
r_A	Reaction rate

r_p	Radius of resin bead
R_e	Equilibrium bubble radius
R_K	Critical bubble radius
Sc_T	Ultrasonic Schmidt number
t	Time
T	Temperature
$t_{1/2}$	Half-life
U	Time mean velocity
v	Velocity
v_B	Bulk kinematic viscosity
v_o	Maximum velocity
V_l	Volume of liquid
W_s	Weight of resin particles
X	Ration of species A adsorbed to species A fed
x, y, z	Cartesian space coordinates

Greek Letters

α	Absorption coefficient
α_{cl}	Classical absorption
α_s	Absorption coefficient in a liquid from frictional losses
α_{th}	Sound absorption coefficient
ε	Void fraction in the resin bed
γ	Ratio of pressure and volumetric heat capacities
η	Viscosity
η_B	Bulk viscosity
η_L	Liquid viscosity
η_s	Shear viscosity

λ	Wavelength
π	Pi
ρ	Density
ρ_A	Density of species A
σ	Surface tension
τ	Shear stress

Abbreviations

ADC	Analog digital converter
CFC	Chlorofluorocarbon
Ci	Curie
ft^3	Cubic feet
gal	Gallon
Ge	Germanium
keV	Kilo-electron volts
kHz	Kilo Hertz
MeV	Mega-electron volts
MW	Molecular weight
sec	Seconds
SRP	Savannah River Plant
yr	Year

1. INTRODUCTION

Throughout the United States, borosilicate Raschig rings were commonly used for nuclear criticality control at DOE Nuclear Facilities between the period of 1950 to 1970 [1] The boron incorporated in the Raschig rings absorbs neutrons released from fissile materials in solution; while the Raschig rings are used for the associated high surface area [2] Guidelines still exist for the use of borosilicate Raschig rings for nuclear criticality control, however, safe engineering design features have become the preferred mechanism for nuclear criticality control of fissile solution storage and processes [3]. The criteria for Raschig rings to completely fill tanks and other voids that could potentially pose a nuclear criticality hazard has led to the generation of large volumes of low-level, high-level, and transuranic radioactive wastes. There is no accurate estimate of the total volume of Raschig rings that are radioactively contaminated and require disposal, however, a reasonable assumption could place the estimate at several thousand 55-gallon drums. Therefore as a result of past nuclear operations, these Raschig rings now compose a radioactive waste stream that poses a significant waste disposal dilemma.

Due to the large volumes occupied by these Raschig rings, decontamination of the rings could potentially be a viable and cost effective method for remediation of this radioactive waste stream. Radioactive waste streams such as contaminated Raschig rings can be broken down into three general categories for disposal 1) low-level radioactive waste, 2) high-level radioactive waste, and 3) transuranic waste The disposal costs

1

depend directly on the classification of radioactive waste stream (i.e., low-level, high-level, transuranic waste). An estimate was made to show the potential economic benefit of remediating radioactive low-level and transuranic contaminated Raschig rings in Figure 1.1. For the qualitative estimates, a base cost of $25/ft^3$ was used for Class A low-level waste while $750/ft^3$ was used for transuranic waste [4,5]. These rough estimates were generated from discussions with industry professionals that deal in the changing environment of radioactive waste disposal.
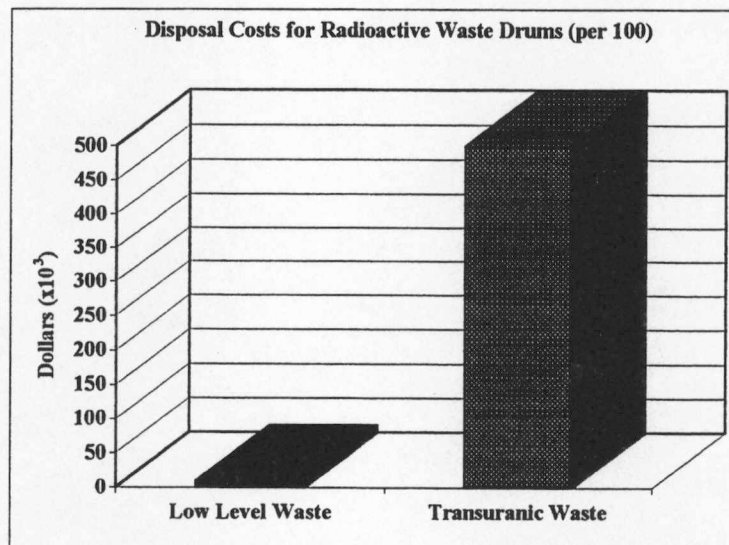
Figure 1.1 Approximate disposal costs of 55-gallon drums of low-level and transuranic wastes.

The relative differences in costs are primarily associated with the restrictions placed on the availability of space for disposal and associated handling costs. The disposal costs for transuranic wastes are approximately thirty times greater than the costs for disposal of low-level waste. An accurate number for high-level waste is not currently

available, as the proposed disposal site is not operational   However, a safe assumption can be made that the disposal costs will be equivalent or greater than the disposal costs for transuranic waste.

A focused study was conducted on a uranium-233/thorium-229 radioactive Raschig ring waste stream at the Radiochemical Development Facility at Oak Ridge National Laboratory (ORNL). This specific waste was chosen to develop a methodology that could be applied to other similar radioactive contaminated Raschig ring waste streams   Other Raschig ring wastes contaminated with uranium, thorium, and plutonium would have similar historical process backgrounds and therefore could utilize the results of the remediation approaches developed here for potential application to these wastes

For this particular Raschig ring waste stream, a secondary objective was to recover a valuable but previously undesired isotope (i.e , thorium-229) for ongoing alpha radioimmunotherapy research [5-9]. Alpha radioimmunotherapy is the medical application of alpha emitting isotopes in conjunction with monoclonal antibodies. The alpha emitting isotope is attached to the monoclonal antibody and injected into the bloodstream. The antibody attaches to a tumor cell for which the antibody was designed to have an affinity. At this point the attached radioisotope decays and releases the alpha particle onto the tumor cell   The relative size and associated electrical charge of the alpha particle results in significantly more damage to the tumor cell than conventional radiation therapies that use beta or gamma rays

2.   LITERATURE REVIEW

2.1   RADIOACTIVELY CONTAMINATED BOROSILICATE RASCHIG RINGS

Borosilicate Raschig rings were commonly used from the 1950s through the 1970s to prevent the potential of inadvertent nuclear criticalities in tanks containing fissile solutions.   Therefore, the majority of information generated during that period was directed towards the safe and effective use of borosilicate Raschig rings for nuclear criticality control   There are several papers for the safe use, inspection, and criticality assessment of Raschig rings [1-3]   However, only a limited amount of information was found on the remediation of the Raschig ring waste streams that have been generated over the past thirty years.

Until the start of this research project, little had been published on methods for remediation of radioactively contaminated Raschig rings   This can probably be attributed to the much larger problem of remediation of the radioactive liquid/sludge contents that exist in the same tanks as the Raschig rings   However, this oversight to investigate methods for remediation of radioactively contaminated Raschig rings does not solve the problem of disposal and remediation of these Raschig ring waste streams.

Without a method of treatment for radioactively contaminated Raschig rings, proper disposal would be to package the rings in drums and dispose of the drums at approved burial sites.   However, due to the associated costs per volume for transuranic

(and high-level) wastes, traditional methods of disposal may be expensive for many of the waste streams

Another published method was performed in 1978 in Germany [10] During the decontamination of various process cells, eighteen vessels were emptied of boron glass Raschig rings and conditioned for waste packages suited for sea disposal. Currently approved regulations in the United States do not allow for disposal of radioactive materials at sea. Therefore, the relevancy of that work, other than to establish the negligible amount of research performed on remediation of radioactively contaminated Raschig rings, is limited.

In the United States, concurrent to the initiation of this research project was the development of a Raschig ring remediation study at the Rocky Flats Environmental Technology Site [11]. The preliminary study recommended a remediation technology that utilized a combination of nitric acid and ultrasonic agitation Additional information concerning application of the study was not found

2.2 BACKGROUND INFORMATION

2.2.1 ORNL Uranium-233/Thorium-229 Raschig Ring Waste Stream

The particular Raschig ring waste stream addressed in this study was a remnant of a uranium/thorium separation process conducted at ORNL in the 1970s The process was used to separate uranium-233 and uranium-232 from their associated decay products. The primary decay products of concern are the first daughters, thorium-229 and thorium-228, due to their dominant half-lives (7,430 years and 1 8 years respectively). The

5

original process involved a nitric acid dilution of the uranium feedstock followed by a cation ion exchange process where the resin had a higher selectivity for thorium than for uranium. The thorium was then eluted with an ammonium acetate complex. The eluant, with slight uranium contamination, was stored in a vessel filled with borosilicate Raschig rings for several years before the material was disposed [12] This left approximately seventy cubic feet of radioactively contaminated borosilicate Raschig rings. The Raschig rings were stored in the tank until 1993, when the Raschig rings were vacuum extracted and transferred to 55-gallon drums

The Raschig rings were recovered during 1993 in an effort to retrieve any residual thorium-229 that remained in the tank and on the Raschig rings As mentioned earlier, thorium-229 has been identified as a potential parent isotope for a new method to treat various bloodborne tumors [5-9] The additional potential of recovering an identified valuable product from what would otherwise be considered a waste provided the economic motivation for the project

2.2.2 Project Outline

The difficulty of establishing a successful remediation or treatment process for heterogeneous high-level radioactive waste has been the subject of other research projects [11,13-14] Prior to the start of this project, the only data that existed on contaminant extraction of the selected Raschig ring waste stream was provided by ORNL's Radiochemical Analytical Laboratory [15]

Four heterogeneous samples had been retrieved and sent for isotope and chemical analysis The samples were pulled randomly from the Raschig rings near the bottom of the waste storage vessel The decision to pull samples from this location in the vessel was based on the assumption that the highest concentrations of thorium-229 were present near the bottom of the tank Surface radiation levels from the Raschig rings extracted from this region validated the assumption that concentrations were higher at the bottom of the tank This assumption should also be typical of a waste tank with sludge or sediment that had settled to the bottom of the tank

The following is an outline provided by the Radiochemical Analytical Services at ORNL of the basic steps used to recover the contaminants from the Raschig rings [16].

- The Raschig rings were submersed in 100 ml of 3N nitric acid

- A magnetic stirrer was used to mix the solvent, and the temperature was raised to ~ 80 °C

- Up to several milliliters of 5N hydrofluoric acid were added to assist in the removal of the contaminants.

- The recovery process was continued for a period of approximately 48 hours

The use of hydrofluoric acid and the time that was reported to recover the contaminants illustrates the basic assumptions concerning the difficulties expected in remediating the Raschig ring waste stream

2.3 Glass Cleaning Technologies in Other Industries

Borosilicate Raschig rings are glass cylindrical rings with a high concentration of boron in the glass matrix A literature review of industry technology and standards for glass cleaning in other industries found significant information on a wide range of techniques but no direct applications to the remediation of radioactively contaminated borosilicate Raschig rings. The following is a brief overview of the areas and information available that provided insight into similar applications.

The American Society for Testing and Materials publishes a standard, *Practice for Designing a Process for Cleaning Technical Glasses* (C912) [17], which provides guidance for development of a process for cleaning glass substrates.   Common applications are pharmaceutical, computer, telecommunications, and research laboratory industries

Somewhat more relevant to this project, a method for cleaning borosilicate glass for biological applications was developed by Pantano and Hench that used various surfactants and ultrasonics to clean borosilicate glass of several petroleum based organic compounds [18]

Harding performed a study evaluating methods to remove oil and grease contaminants from glass for the semi-conductor industry.   Harding studied the effectiveness of common water based surfactants as replacement alternatives for CFC and trichloroethylene, which are being phased out of use because of their detrimental effects on the environment [19]   The study utilized a 40 kHz ultrasonic sink and glass

microscope slides contaminated with various oil and grease compounds   Harding concluded that the surfactants were not as effective as traditional cleaning agents on the oil and grease contaminants   However, his results could be considered successful if applied to a waste remediation project where the final results were not as stringent

A similar study was performed by Slanina to evaluate the effectiveness of spray cleaning circuit boards with several aqueous cleaning detergents [20]   The study had a similar conclusion as Harding on the relative ineffectiveness of the proposed cleaning alternative to standard methods   However, this report provides a viable alternative to ultrasonics for remediation of a waste stream where once again the criteria for cleanliness are not as critical as in the circuit board manufacturing industry.

Gollapudi (et. al.) performed an ultrasonic treatment study for the removal of asphaltine deposits on glass substrates [21]   The ultrasonic mediums were either aqueous or kerosene. The key parameter evaluated in this investigation was the effect of frequency on the cleaning effectiveness

Additional information on ultrasonic cleaning of glass with acid and surfactants was found in an article in *Glass* [22]. The article provided lessons-learned on various applications of ultrasonics, acids, and surfactants. The key recommendation on surfactant selection was to choose a low foaming, alkaline, easily rinseable agent. This criteria led to the selection of the surfactant, with the trade name Simple Green™ manufactured by Sunshine Makers, Inc for remediation experiments of the radioactively contaminated borosilicate Raschig rings.

2.4 Regulatory Requirements

There are three types of radioactive wastes that were used to provide the basis for this project: 1) low-level waste, 2) high-level waste, and 3) transuranic waste Low-level waste is defined as waste that contains radioactivity and is not classified as high-level waste, transuranic waste, or spent nuclear fuel or byproduct material as defined in section 11 e.(2) of the Atomic Energy Act of 1954 (42 U.S C 2014(e)(2)) [23] High-level waste is defined by the Nuclear Waste Policy Act of 1982 as the highly radioactive material resulting from the reprocessing in the United States of spent nuclear fuel, including liquid waste produced directly in reprocessing and any solid material derived from such liquid waste that contains fission products in sufficient concentrations; the highly radioactive material resulting from atomic energy defense activities, and any other highly radioactive material that the Commission, consistent with existing law, determines by rule requires permanent isolation [24]. Transuranic waste is defined by 40 CFR 191 as waste containing more than 100 nanocuries of alpha-emitting transuranic isotopes, with half-lives greater than twenty years, per gram of waste, except for: (1) High-level radioactive wastes, (2) wastes that the Department has determined, with the concurrence of the Administrator, do not need the degree of isolation required by this part, or (3) wastes the Commission approves for disposal on a case-by-case basis per 10 CFR Part 61 [25].

These regulatory definitions provide the design basis for the experimental and application studies to determine whether the radioactively contaminated Raschig rings can be decontaminated sufficiently to meet the definitions of the waste classification

3. EXPERIMENTAL

The residual radioactive contamination on the Raschig rings is a direct result of the process from which the Raschig rings were originally utilized Noncontaminated Raschig rings are shown in Figure 3 1 and provide a baseline for visually comparing the effectiveness of the remediation processes. Typically, the radioactive contamination on the Raschig rings varies from a thin dry film to a sludge-like material that completely envelops the ring (Figs. 3 2-3.3). However, by considering the process that led to the generation of the waste stream, a remediation scheme can be proposed for effective removal of the radioactive contaminants from the Raschig rings (Fig. 3.4) [5]

The selected Raschig ring waste stream originated from a nitric acid dissolution process; therefore, a nitric acid/ultrasonic remediation method was selected to test its effectiveness in the remediation of the Raschig ring waste stream. Concurrent to the development of this methodology, Raschig ring remediation with nitric acid and ultrasonic agitation was also recommended for the Raschig ring waste streams at the Rocky Flats Environmental Technology Site [11]

As an alternative to the use of concentrated acids, surfactant/ultrasonic agitation was investigated as a technique to remove the radioactive contaminants Numerous industrial and household surfactants are available to clean glass (e.g., Windex®, Formula 409®) Furthermore, an industry exists to develop products and techniques for
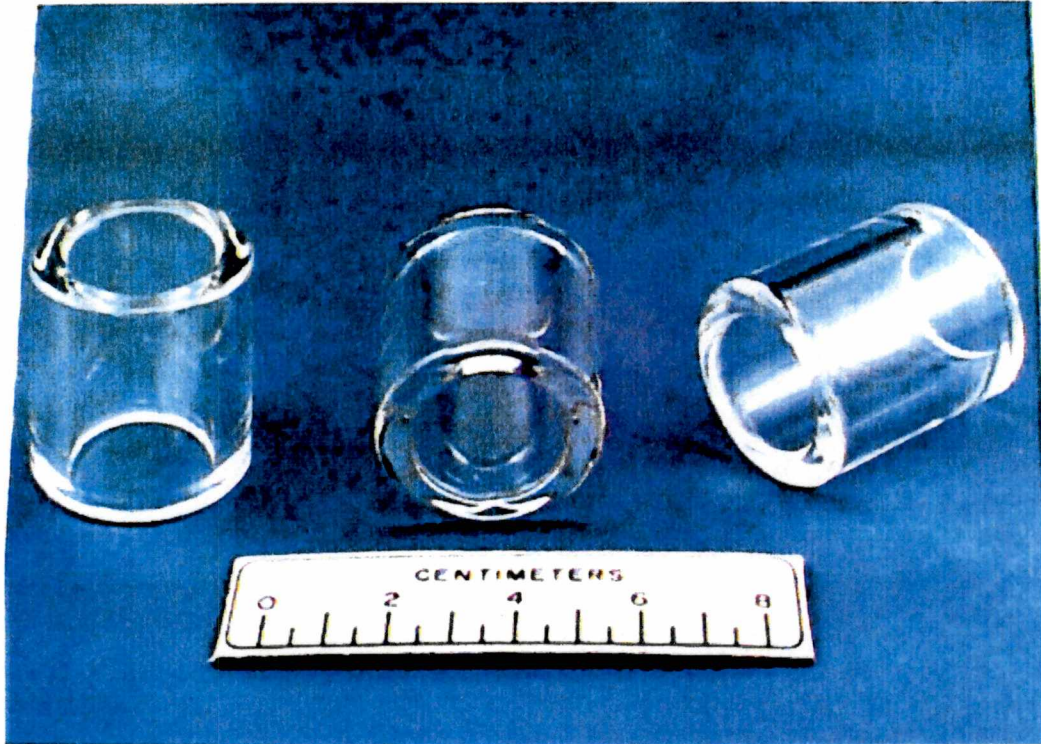
Figure 3.1 Clean borosilicate Raschig rings.

Figure 3.2 Radioactively contaminated borosilicate Raschig rings with thin dry film of contamination.

Figure 3.3 Radioactively contaminated borosilicate surrogate Raschig rings with thick sludge contamination.
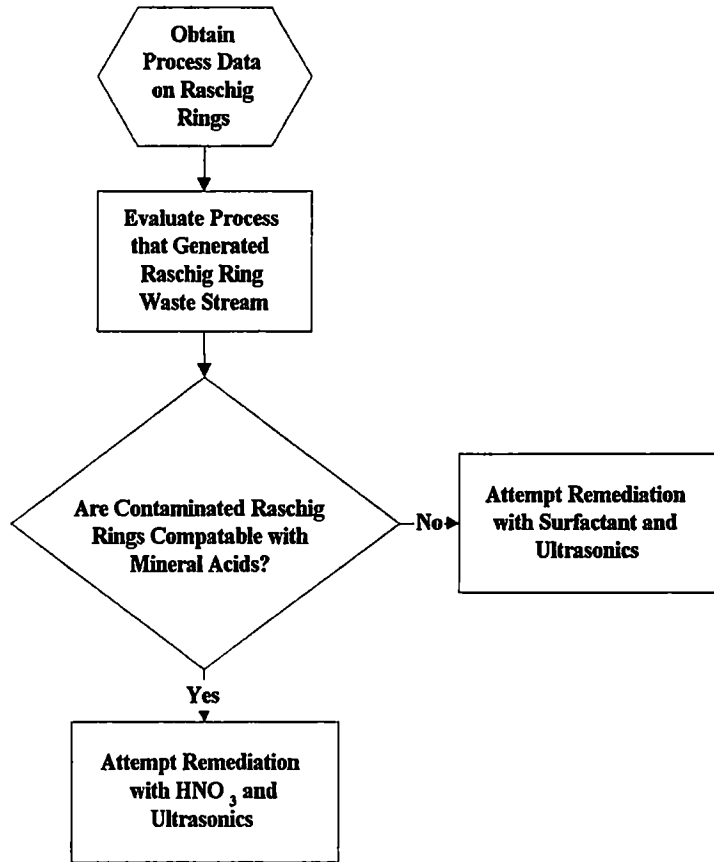
Figure 3.4 Basic schematic for determining a method for remediation of contaminated Raschig rings.

cleaning various types of glass (i e, windows, windshields, optical glass)   For this experiment, a common bio-degradable surfactant was chosen to study remediation effectiveness on contaminated Raschig rings   The effectiveness of the surfactant was then compared to the nitric acid results

Contaminant removal is the first step in a remediation system for Raschig rings The next step is to concentrate the contaminants. Ion exchange separation was chosen as the method to remove the heavy metals, to recover the nitric acid for recycle, and concentrate the radioactive constituents. Both cation and anion ion exchange resins were used to separate and purify the radioactive contaminants   In addition, both batch and column ion exchange systems were tested   For comparison, the contaminated surfactant solution was reduced in volume by evaporation to form a solid salt cake

3.1 RASCHIG RING REMEDIATION TESTS

The Raschig ring remediation studies were separated into four phases (1) baseline evaluation of the effectiveness of deionized water as a solvent, (2) nitric acid remediation study of the effect of temperature and acid normality; (3) a combination of ultrasonic/surfactant remediation tests to evaluate the potential for alternative cleaning techniques and provide for the development of a economic evaluation between the nitric acid method and surfactant method, and (4) remediation of the Raschig rings without the use of ultrasonics to isolate the mass transfer removal contributions.   The general experimental procedure and supporting data are shown in Appendix B

16

3.1.1 Baseline Raschig Ring Remediation Data

Baseline metal analyses of the residue on the selected Raschig ring wastes are shown in Tables 3 1 and 3.2 The source of the samples for Table 3.1 was residue recovered from material obtained from the bottom of the Raschig ring vessel. The samples for data in Table 3 2 were residues from Raschig rings recovered throughout the vessel The variations in the two analyses can be attributed to the heterogeneous nature of the waste stream Also, from the data an assumption can be made that the dominant species present is natural thorium (i e , thorium-232), which was added to the original process during flushing operations of the system.

Initial remediation experiments were conducted with a mechanical stirrer and deionized water at room temperature (Fig 3 5) The data provided a baseline against which to compare the effectiveness of the subsequent nitric acid/ultrasonic and surfactant/ultrasonic experiments Remediation with water and the stirrer was surprisingly effective given the reported difficulty from previous attempts reported in Section 2.2.2.

To isolate the mechanically induced mass transfer effects, two additional baseline experiments were performed to measure the remediation effectiveness of the nitric acid and the surfactant Raschig rings were submerged in either nitric acid or surfactant to establish the remediation rate due to chemical dissolution of the contaminants (Figs 3 6 and 3 7). Multiple experimental runs were conducted with various nitric acid concentrations to verify the effects of the nitric acid on the remediation rate. The slow rate of dissolution from the nitric acid alone establishes the significant effect of

Table 3.1 Metals analysis of Raschig ring residue provided by the Institute for Transuranium Elements.

Species	Concentration (μg/ml)	Species	Concentration (μg/ml)
Al	30 70	Sn	0 129
B	0 516	Mo	0.258
Cr	7 482	Ba	0 129
Cu	1.29	Pb	40 76
Fe	114 04	Ta	0.0516
Mg	4.90	Cd	0 129
Mn	1.29	Gd	< 0.077
Ni	10 3	W	< 0 077
Th 232	2580	Sr	< 0.077
Ti	0 516	Sb	< 0.077
U 233	622	Zr	0 129
U 238	5 4	Nb	0.258
Zn	2.06	Th 229	21.67

Table 3.2 Metals analysis of Raschig ring residue provided by Oak Ridge National Laboratory

Species	Concentration (μg/ml)	Species	Concentration (μg/ml)
Ag	0.280	Mg	< 0 197
Al	393	Mn	2 75
Ba	< 0 014	Na	740
Be	0 08	Ni	2.57
Ca	32.7	Sb	< 2.20
Cd	< 0 220	Th (total)	2580
Co	< 0.144	Th-229	⁻1 1
Cr	4.38	U	180
Cu	2 14	V	0.320
Fe	364	Zn	45 4
K	18 3		

Remediation Rate for Borosilicate Raschig Rings in H_2O
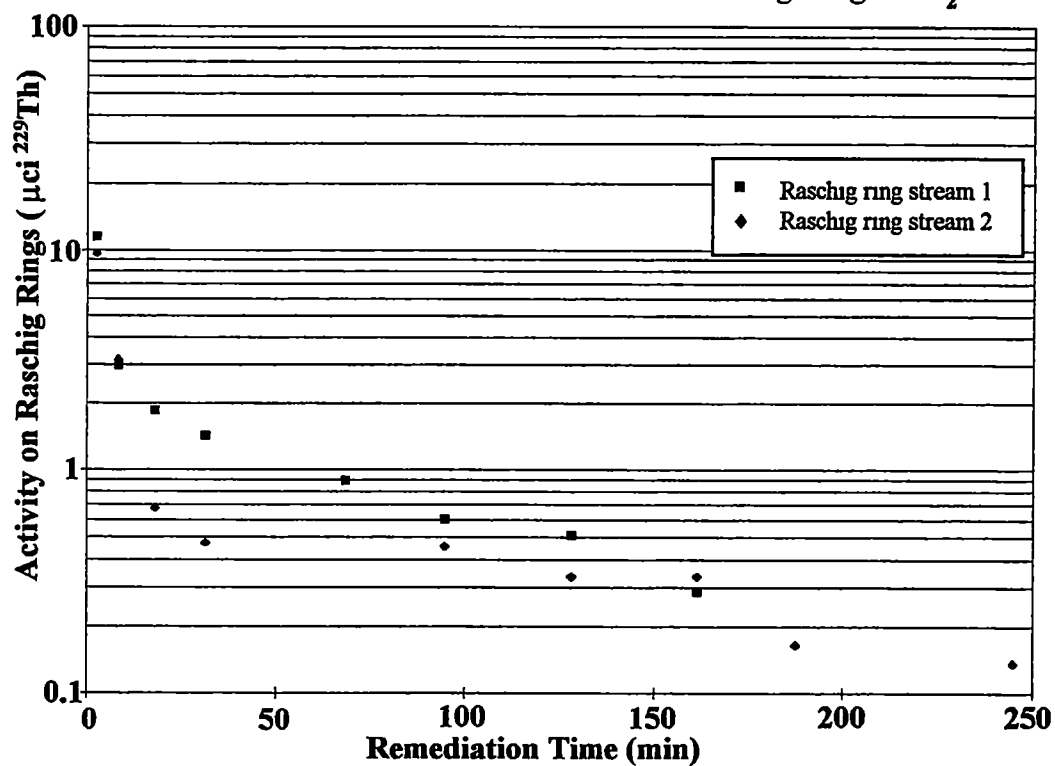
Figure 3.5 Remediation rate for two independent waste streams of radioactively contaminated borosilicate Raschig rings with deionized water and mechanical stirrer agitation.
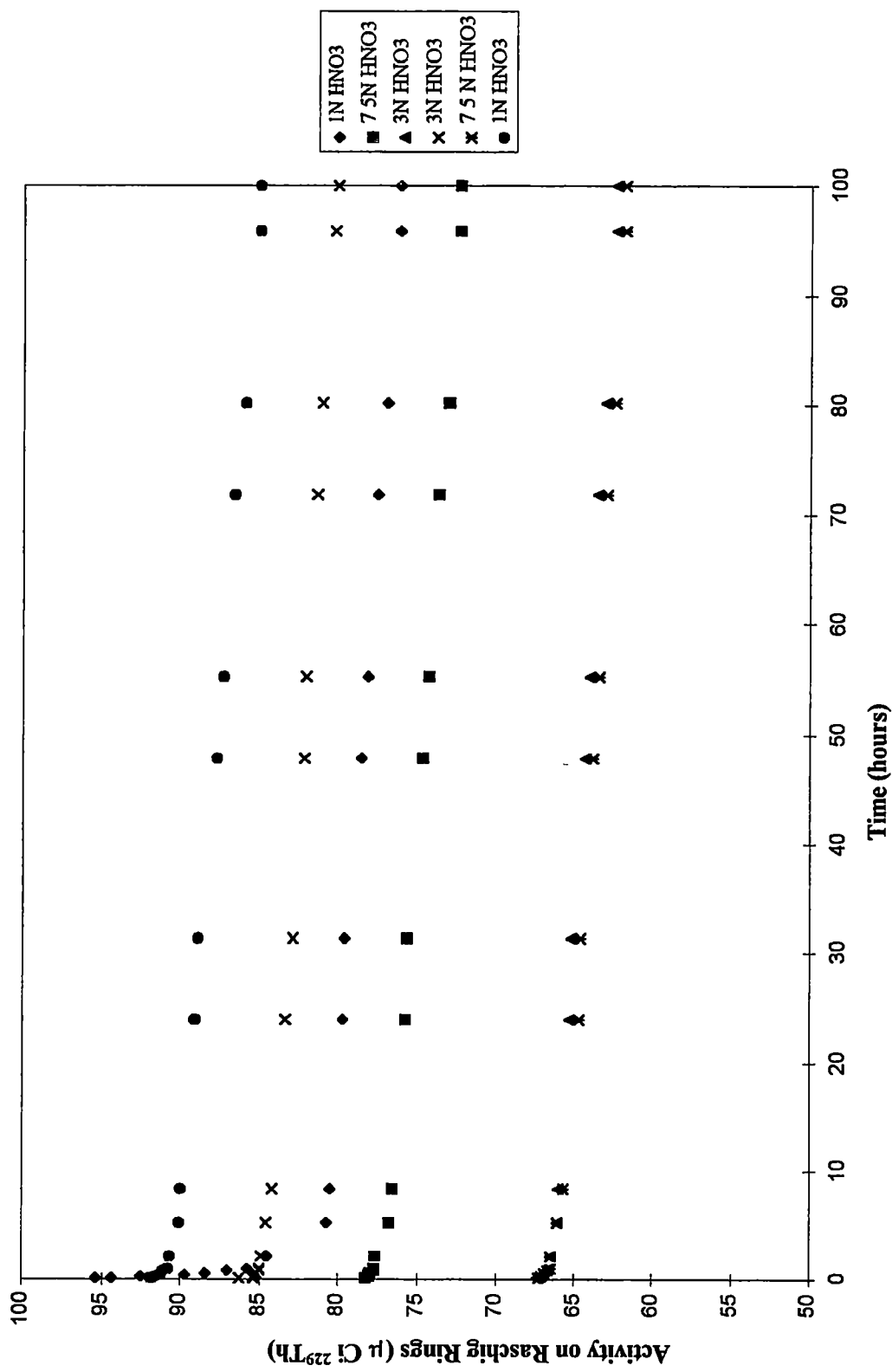
Figure 3.6 Remediation rate for borosilicate Raschig rings in HNO_3 and no mechanically induced agitation.

21
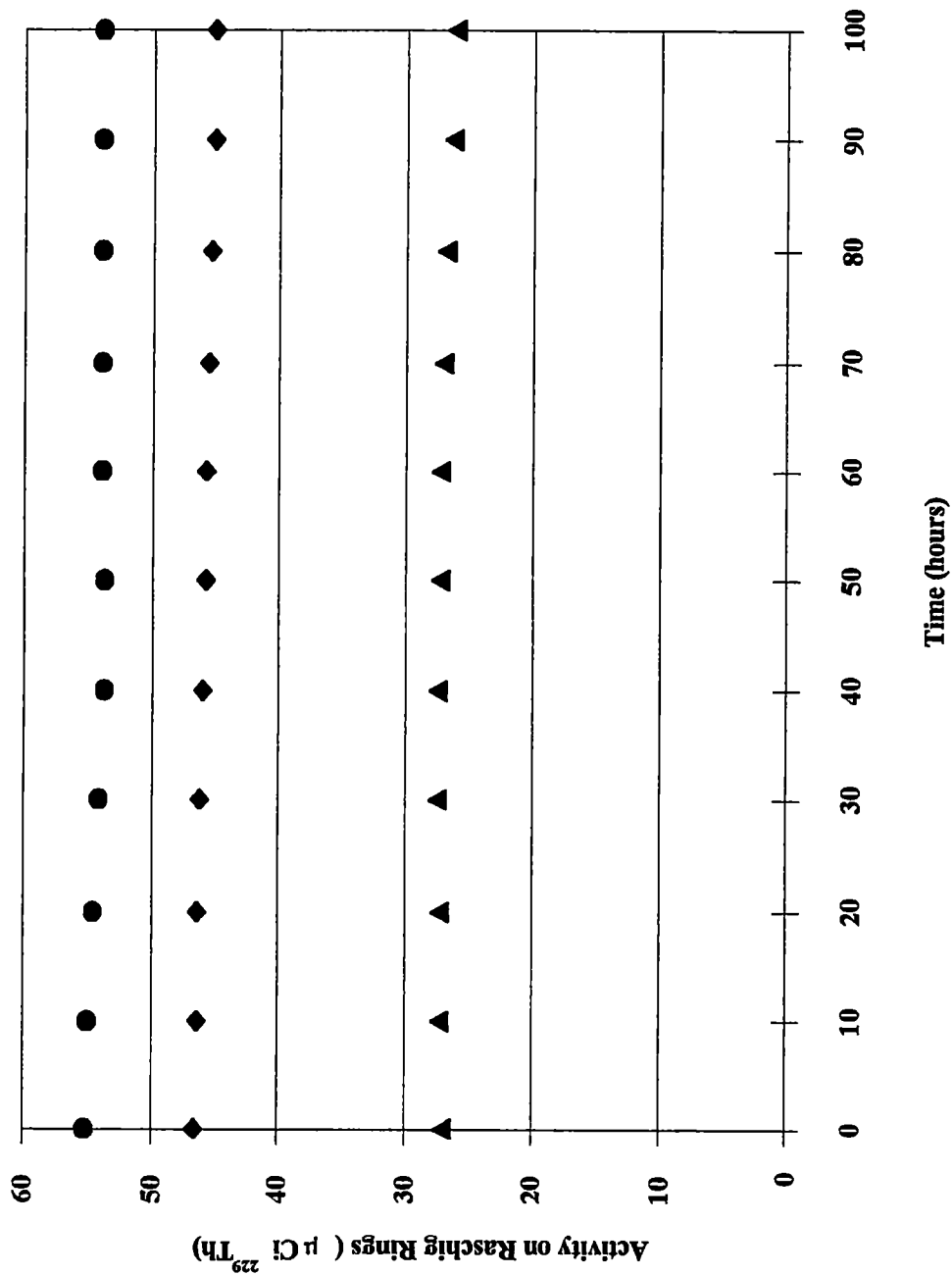
Figure 3.7 Remediation rate for borosilicate Raschig rings in surfactant (Simple Green™) with no mechanically induced agitation.

the increased mass transfer associated with the mechanical agitation. For the experiments conducted, successful remediation could be extrapolated to a transuranic waste stream, as long as, the average transuranic curie concentration was below approximately 5 8 μCi/Raschig ring, where 5.8 μCi/Raschig ring is equivalent to the regulatory limit of 100 nCi/gm of transuranic waste. From the results in Section 3 and the data files in Appendix B, the treatment of a transuranic waste to low-level waste would have been easily achieved

The effectiveness of the remediation was measured through gross gamma radiation measurements and gamma spectroscopy Gamma spectroscopy was used to determine the activity of the primary isotope that remained on the Raschig rings (i.e., thorium-229). The gamma spectroscopy unit also provided specific characterization of the decay products A description of the fundamental operation of a gamma spectroscopy unit is provided in Appendix A This analytical method was chosen to provide discrete and rapid determination of the radioactive constituents and associated decay products that undergo a gamma decay (e g , uranium-233, uranium-232, thorium-229, and thorium-228)

The sequence of operations began with a calibrated gamma spectroscopy unit with known sample geometry and calibrated gamma sources. The sample was counted for approximately fifteen minutes, at which time the curie activity of the thorium-229 isotope was determined by the yield of the 193 keV and 210 keV gammas from the decay of thorium-229 The thorium-229 concentration was then determined from the quotient of the thorium-229 activity and the specific activity The thorium-229 concentration could

23

then be correlated to the total thorium concentration through a ratio developed from isotopic analysis The frequency of the measurements was then acquired from trial and error to find the optimum interval for successful remediation.

3.1.2   Nitric Acid Remediation Tests

The nitric acid remediation tests were conducted to establish the effectiveness and an optimum operational region for remediation of the contaminated Raschig rings. The two key process variables modified were temperature and nitric acid concentration with a constant applied frequency and intensity from the ultrasonic generator Nitric acid was chosen based on previous process knowledge associated with the waste stream and to minimize the corrosive effects on the process equipment (e g , ventilation and laboratory hoods) that are typically associated with the use of hydrochloric or sulfuric acids. Remediation tests indicated minimal effect from change in temperature and nitric acid concentration of the remediation time (Fig 3 8).

The minimal effect of temperature and nitric acid concentration on the remediation time of the Raschig rings is overwhelmed by the more dominant effect of the ultrasonic agitation.   This is seen later when the remediation time is compared to the surfactant/ultrasonic experiments in section 3 1.3.

3.1.3   Ultrasonic/Surfactant Tests

Experiments were conducted to establish an alternative remediation technique and determine the relative effectiveness of the nitric acid remediation method   A commercially

24
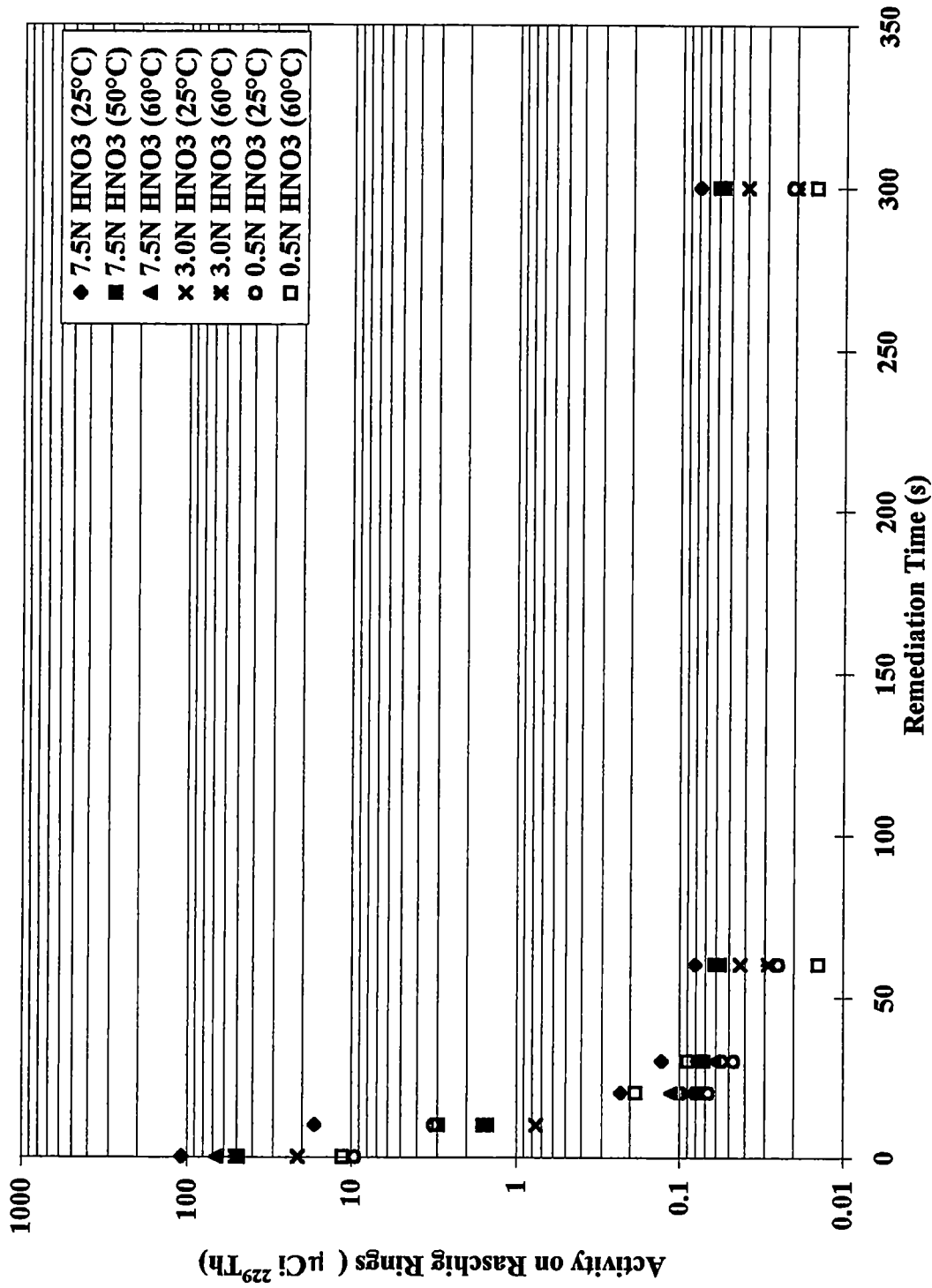
Figure 3.8 Effect of various temperatures in HNO_3 with ultrasonic agitation on remediation rate.

25

available surfactant, by trade name of Simple Green™, was used for the remediation studies The choice of the surfactant was based on the bio-degradable classification of the surfactant and the economical aspects that could be applied to a larger scale operation The bio-degradable classification should ensure the secondary waste meets established land disposal restrictions for radioactive wastes. The temperature was ambient, ~25°C, and the ultrasonic frequency was fixed at 55 kHz and with power at 120 watts (0.6 watts/ml). The resultant radioactively contaminated solution was reduced in volume by evaporation to a salt cake The volumetric reduction of the solution was approximately 10.1. There was no apparent degradation of the cleaning effectiveness of the surfactant after twelve successful remediations or approximately 1 cubic foot of Raschig rings per 0.3 liters of solution This would allow the surfactant to continue to be used for multiple decontamination efforts Of course, the effectiveness of the surfactant will be a function of the material deposits on the Raschig rings Figure 3.9 compares the remediation times for the surfactant tests to the remediation times from the 7.5N nitric acid tests. The experimental procedure is described in Appendix B

The relative effectiveness of the 7 5N nitric acid and the surfactant remediation ultrasonic methods was essentially equivalent as seen by the final concentrations of contaminants on the Raschig rings However, one key difference in the remediation techniques was the removal of the yellowish stain on the Raschig rings, seen in Figure 3 2, with the surfactant method Another difference is the relative hazards associated

Remediation Effectiveness of Surfactant vs. 7.5N Nitric Acid
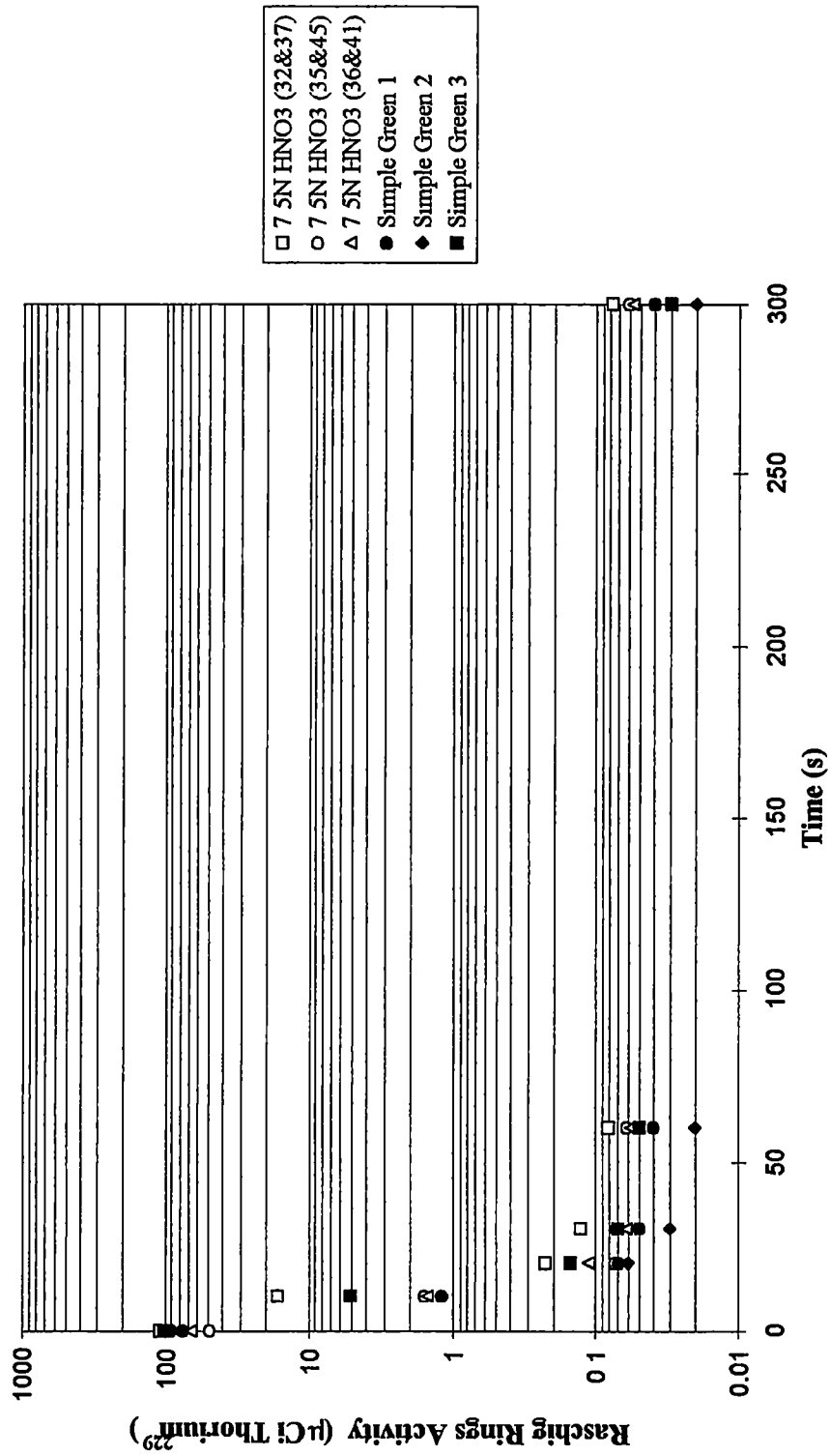
Figure 3.9 Relative remediation effectiveness of surfactant (Simple Green™) vs. 7.5N nitric acid with ultrasonic agitation.

with an acid process are substantially reduced with the use of a biodegradable surfactant

This factor becomes significant in the economic analysis of process scale-up

Evaporation of the contaminated surfactant was performed to establish a volume reduction step for the contaminated remediation solutions The volume reduction for the laboratory trials was performed by heating the waste solution to 100°C. As the solution evaporated, the solutes concentrated into a salt cake. The average reduction in solution volume was 10 1 from the initial volume The time to evaporate the samples and the volume reductions are given in Table 3.3. The residual solids were defined as "dry" after no freestanding liquid was visible The final dried volume in Table 3 3 was primarily due to the solidification of the dissolved solids in the surfactant. Therefore, the actual volume reduction on a larger scale would be the summation of the contaminants on the Raschig rings with an estimate of a factor of ten reduction from the initial surfactant volume.

Table 3.3   Volumetric reduction data for Raschig ring surfactant remediation experiments.

	Initial Solution Volume (mls)	Raschig Ring Volume (cm^3)	Final Dried Volume of Solution (cm^3)	Volume Reduction Ratio	Time (hrs) @ 100°C
Run 1	300	28,317	32	9.4	29
Run 2	300	28,317	31	9.7	31
Run 3	300	28,317	28	10.7	27
Run 4	300	28,317	27	11 1	28
Run 5	300	28,317	33	9 1	32

If the results of the remediation with the surfactant method were applied to a similar waste stream that was contaminated with a transuranic waste, the overall reduction of the transuranic component would be over 800:1 based on the removal of the contaminants and the resultant volume of the salt cake Furthermore, volume reduction of the decontaminated Raschig rings by crushing would reduce the final volume of the Raschig rings to ~ 50% of the initial volume.

Prior to beginning the surfactant experiments, the potential problem of surfactant foaming was of concern Generation of foam during ultrasonic agitation would present an operational problem for the surfactant method of Raschig ring remediation However, during all Raschig ring remediation studies with the Simple Green™ surfactant no foam was observed.

3.2 ION EXCHANGE SEPARATION EXPERIMENTS

For this project, the contaminants were separated via a batch ion exchange method Initial attempts were made to utilize a gravity ion exchange column, however, the significant quantity of particulate matter required a filtration step prior to ion exchange column separation The gravimetric filtration method utilized to filter the feed material was a labor-intensive effort The difficulty of filtration on the laboratory scale was noted as a problem to be considered in engineering design for potential scale-up of the process

29

Due to the radioactive hazards associated with this process, a simplistic method was developed for batch ion exchange separation This eliminated the need for the feed filtration step and allowed the process to be performed in steps without continuous operational coverage. This approach minimized worker time in direct contact or vicinity of the feed material, which reduced the hazardous exposure to the operational personnel. However, the lessons obtained from this process emphasize the need for adequate filtration in the design of a larger scale Raschig ring remediation process that utilizes ion exchange separation

3.2.1   Anion Ion Exchange Batch Separation Data

The dissolved contaminants were separated from the nitric acid solution by batch anion exchange. The primary contaminant of interest was thorium (see Tables 3.1 and 3 2) The thorium was desired for use in the advanced alpha radioimmunotherapy medical studies

For the anion ion exchange separation studies, the proposed dominant thorium complex dissolved in a 7 5N HNO$_3$ solution is given by:

$$Th^{+4} + 6HNO_3 \leftrightarrow Th(NO_3)_6^{-2} + 6H^+ \qquad\qquad (3\ 2\ 1)$$
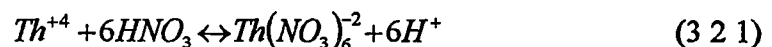
Since most other metal cations do not form anion complexes with nitrate ions, the use of anion exchange results in preferred thorium product relatively free of contaminating ions.

The ion exchange for the thorium nitrate complex is be given by

$$Th(NO_3)_6^{-2} + RNO_3 \leftrightarrow R \bullet Th(NO_3)_6 + 2NO_3^{-2} \qquad (3\ 2.2)$$
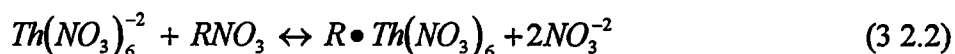
The analytical results for concentration of the thorium-229 species were determined in curies per milliliter, Ci/ml, of sample by gamma spectroscopy. A conversion to grams/ml is performed by calculating the Ci/g, specific activity, of the radioactive species, which is given by

$$Ci\Big/ g_A = \frac{1.13 \times 10^{13}}{t_{\frac{1}{2}}(\text{sec})MW} \qquad (3.2\ 3)$$

For these experiments, the primary radioactive contaminant measured was thorium-229 The ratio for total thorium, primarily thorium-232, to the thorium-229 concentration was developed from initial analytical samples From Tables 3 1 and 3 2, a conservative ratio of grams of thorium-232 to grams of thorium-229 was estimated to be ~ 2000 1.

The normality of one gram of the thorium nitrate complex, $N_{Th(NO_3)^{-2}}$, per liter basis was calculated to be 3 3x10^{-3} eq/gram For the Reillex HPQ™ resin, the exchange capacity was 3 3 meq/g dry resin (data supplied by the manufacturer) From this standard basis value, the minimum grams of dry resin per gram of thorium to be recovered was

31

determined to be 2 61 g dry resin/g thorium.   A typical value of thorium-229 concentration was 9.5 mg/l (Appendix B)   Hence, for 100% loading on the ion exchange resin, a minimum of 24 8 g of dry resin was required per liter per batch ion exchange run   To ensure high efficiency adsorption and enhance mass transfer rates an average mass of 200 g of dry resin was used per 0.5-liter batch run, sixteen times the calculated mass of resin for complete loading   The mass transfer effects were confirmed to be minimized for the 0.5-liter batch anion runs by varying the mass of resin   Up to the 200 g of resin threshold and 250 secs , a linear relationship was seen between the ratio of surface to volume (surface area per volume of solution) and the mass transfer properties (Figure 3 10)

The sequence of operations for the anion ion exchange process began by washing 200 g of dry resin to remove small resin fines and other contaminants   Then the resin was soaked in 7.5N HNO_3 to convert the resin to the nitrate form   The nitric acid solution from the ultrasonic remediation step was heated to 60°C in accordance with the process optimization performed by Rainey [26]   While simultaneously, the resin in the 7 5N HNO_3 was heated to 60°C. Once temperatures stabilized, the nitric acid solution from the ultrasonic remediation step was added to the 7 5N HNO_3 resin and stirred until the thorium nitrate complex was adsorbed, which was confirmed by means of the procedure outlined in Appendix B
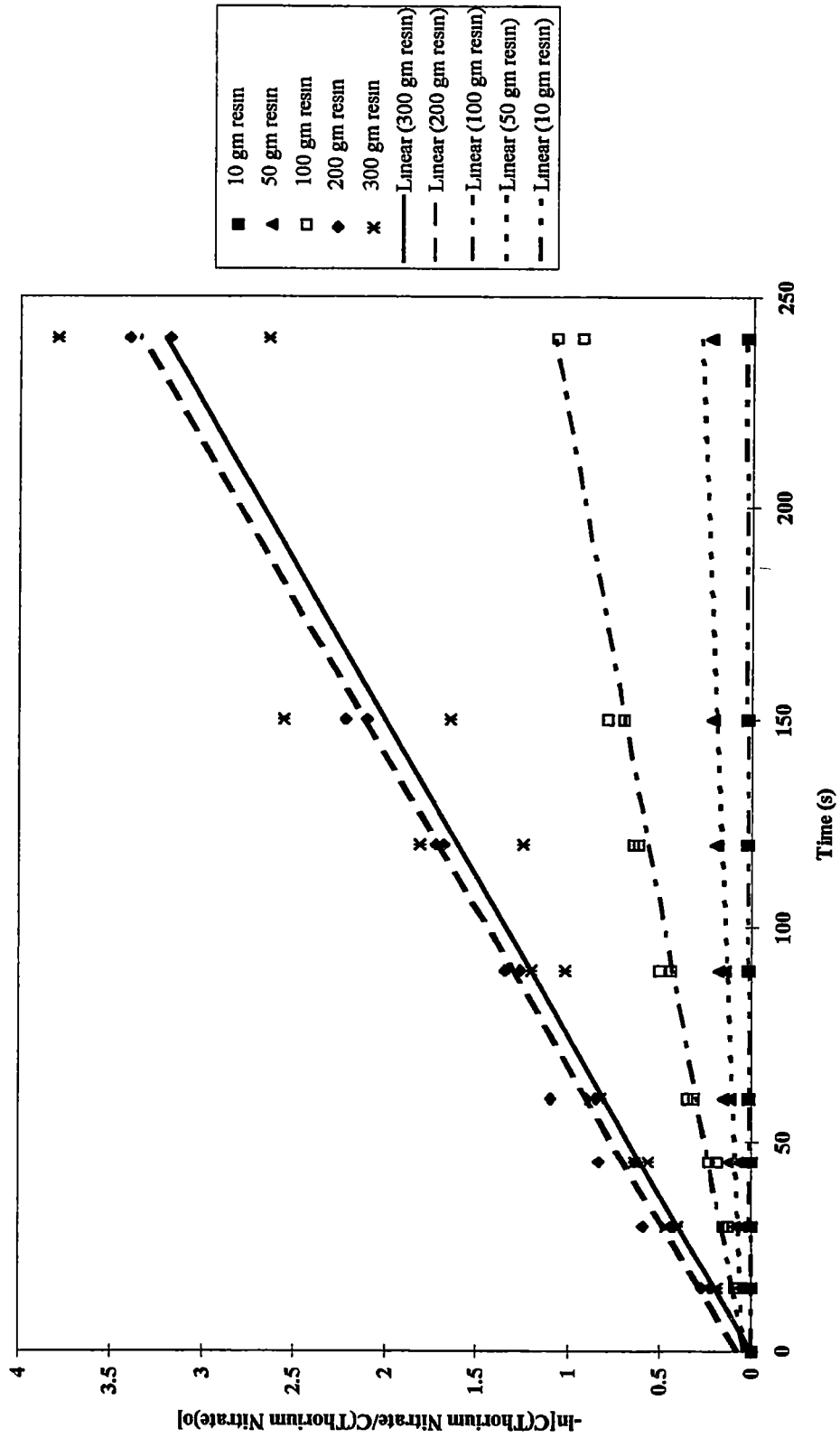
Figure 3.10 Adsorption Rate for thorium nitrate with Reillex ™ HPQ anion ion exchange resin at 60 °C.

33

A plot of Equation 4 2 10 in Figure 3 10, $\ln\left(C_{Th(NO_3)_6^{-2}} / C_{Th(NO_3)_6^{-2}_0} \right)$ versus t,

gives the adsorption rate for the batch ion exchange process   Where, the rate constant, k_A,

for adsorption is found from the slope of the line   Derivation of this model is shown in

Section 4.2

Therefore, the adsorption rate constant for the 200 gm anion resin case, k_A, is

approximately 0 0136 $\sec^{-1}$ Consequently, with a volume for k_A, the concentration at any

time, t, can be found from Equation 4.2.10 to be

$$C_{C_{Th(NO_3)_6^{-2}}} = C_{C_{Th(NO_3)_6^{-2}_0}} e^{-0\ 0136 t} \tag{3.2 4}$$

However, it should be noted that this solution is for the system described by the following

conditions   (1) T = 60°C, (2) 0 5 liter batch in an Erlenmeyer flask, (3) 2" magnetic

stirrer at 50% setting   For similar conditions where excess resin is used to minimize mass

transfer effects the adsorption rate constant and Equation 3.2 4 should be valid   These

conditions optimized the batch ion exchange process to minimize worker radiological

exposure and maximize recovery of the thorium species

In an effort to recover the thorium, the resin was flushed and then filtered with

7 5N HNO_3 to remove residue contaminants   Following the flush, the resin was mixed by

magnetic stirrer in a batch mode with 300 mls to 400 mls of 0.1N HNO_3 to shift the

thorium back to a positive ionic form and elute the thorium from the ion exchange resin

Upon completion of this step, the resin slurry was again filtered and eluted to recover the thorium in solution

3.2.2 Cation Ion Exchange Batch Separation Data

Cation ion exchange was used to purify the thorium recovered from the ultrasonic remediation of the Raschig rings This step was incorporated due to the minute uranium and iron impurities remaining after the anion separation These were the contaminating ions that formed sufficient anion complexes to be removed by the anion resin. Initially, the cation ion exchange separation step was not planned due to the difficulties in separating the thorium species from the cation resin For most applications to larger scale Raschig ring remediation projects the anion separation would have been satisfactory for contaminant removal However, for this project the primary product of interest, thorium, was to be recovered for applications in nuclear medicine research and further purification was required Therefore, the cation ion exchange step was included as an additional purification step in removing the trace metal impurities in the eluant after the anion ion exchange step.

After anion separation, the thorium in a 0 1N HNO_3 solution is primarily a positively charged ionic species Cation resin was chosen for use with the dilute nitric acid solution due to the high selectivity of cation resin for multivalent positive ionic species The relative affinity of the cation resin for Th(IV) is so strong that elution proves to be extremely difficult with variations of nitric acid concentration and temperature [26]

This led to the use of ammonium acetate dissolved in acetic acid to form the following thorium acetate complex.

$$Th^{+4}+4CH_3COONH_4 \leftrightarrow Th(CH_3COO)_4+4NH_4^+ \qquad (3\ 2\ 5)$$
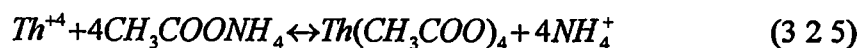
The neutral thorium acetate complex could then be eluted from the cation ion exchange resin. Following the recommendations of Rainey [26], the ideal concentrations of ammonium acetate and acetic acid in the range of 4 to 4 5 M were studied. Throughout the batch process, the temperature was maintained at approximately 60°C [26]. After elution, the thorium acetate was boiled to dryness to convert the thorium acetate to a thorium oxide compound for future chemical separations in support of the medical research applications [5-9]. The quantity of cation resin (AG50W-X12) required for a 0 5-liter batch run with a nominal thorium-229 concentration of 9.5 mg/l was estimated to be approximately 78 gms on a wet basis This assumes a maximum loading of 2.1 meq/gm (supplied by the manufacturer) To improve mass transfer rates, the amount of resin used was increased until no effect from the change in resin concentration was observable This highest removal rate was found at ~200 gms of resin per 0.5-liter batch of solution The adsorption rate for this batch process with various resin concentrations at 60°C is plotted in Figure 3 11.

The slope of the lines in Figure 3 3 are equivalent to the adsorption rate constant, k_A, for the cation ion exchange system at 60°C as presented in Equation 4.2.10.   The

36

Cation Ion Exchange Adsorption Rate
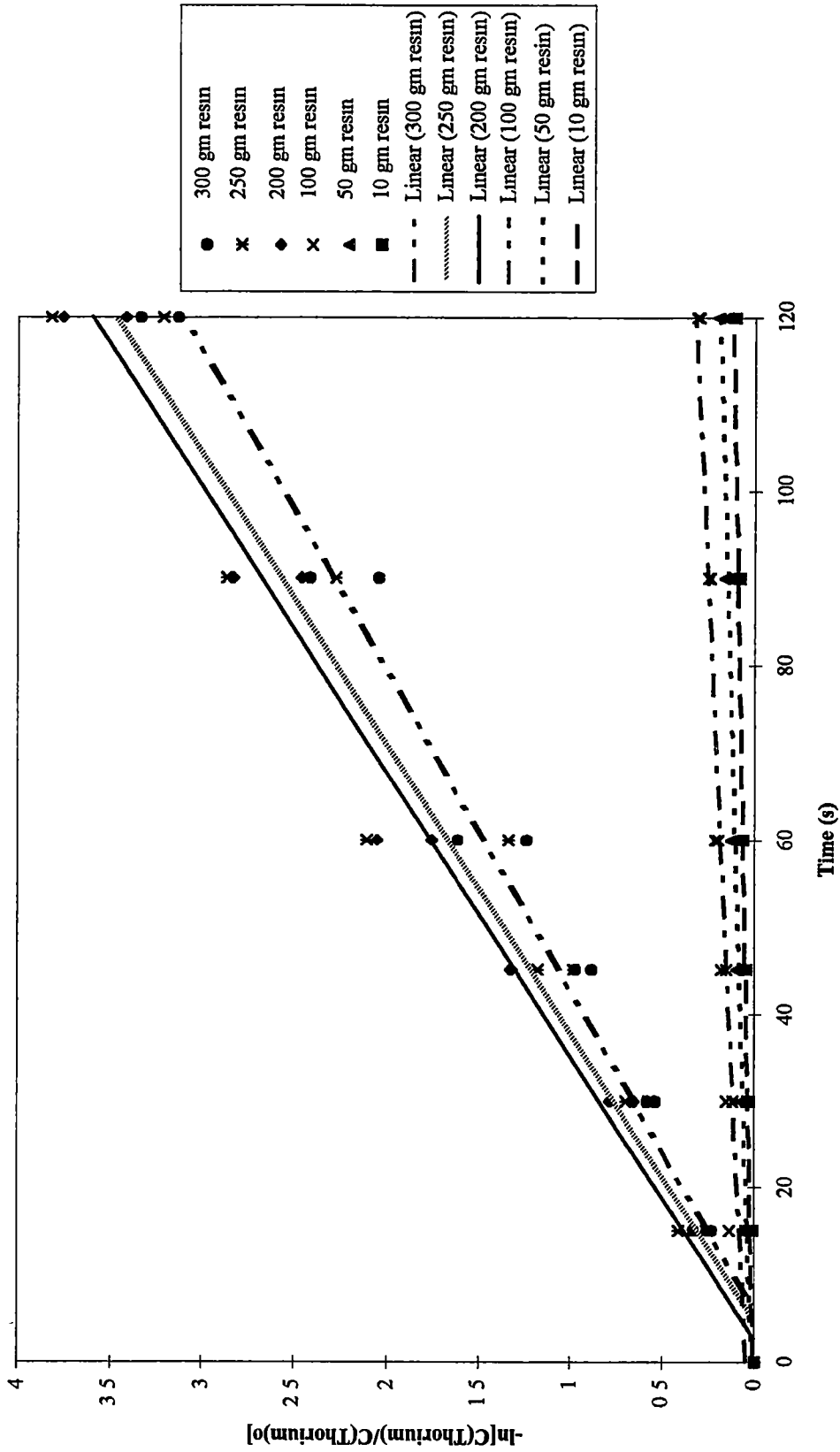
Figure 3.11 Adsorption Rate for Th $^+$ with BIO-RAD AG 50W-X12 Cation Ion Exchange Resin at 60 °C

37

solution for the concentration at time t for the ~200 gram resin loading follows as in Section 3 2 1

$$C_{Th(CH_3OO)_4} = C_{Th(CH_3OO)_4,0} e^{-0\,0307t} \qquad (3.2\ 6)$$

The conditions of the experimental were same as described in Section 3.2 1

4. MODELING OF EXPERIMENTAL RESULTS

From the experimental data, the effectiveness of the remediation was attributed to the mechanically induced agitation Therefore, the mass transfer mechanism is based on the theory for ultrasonic agitation The mass transfer model for ultrasonic agitation provides insight to the physical principals of contaminant removal and justifies the effectiveness of the Raschig ring remediation

The experimental results were divided into two processes (1) a mass transfer model to relate the effects of the ultrasonic agitation versus contaminant removal and (2) an ion exchange model for batch separation of the thorium species. The batch ion exchange model provides the theory for determination of the concentration of the thorium species for an isothermal system The ion exchange process was based on the previous works of Overholt [27] and Rainey [26] The success of the separations confirmed the temperature and solution concentration parameters utilized by Overholt and Rainey.

4.1 ULTRASONIC MASS TRANSFER CORRELATION

Development of a mass transfer correlation for the experimental ultrasonic mass system led to the discovery of a complicated mass transfer process. Experimental equipment limitations of the ultrasonic system (i e., single frequency and power level) prevented an in-depth study of all the mass transfer effects that resulted from the use of ultrasonics combined with the various solvent mediums   However, a detailed development of the ultrasonic theory is presented in Appendix C, which provides the basis

39

for further study into the effects of ultrasonics on mass transfer   A relationship is developed from the ultrasonic theory and dimensionless mass transfer correlations. This relationship was used to hypothesize the effects of changing ultrasonic intensity and frequency

From ultrasonic theory (see Appendix C), a turbulent dimensionless number that provides a ratio of the diffusivity of momentum to the diffusivity of mass due to ultrasonics is the turbulent Schmidt number.

$$Sc_T = \frac{E_{Uv}}{E_D}$$ (4 1 1)

Where,

Sc_T =   turbulent Schmidt number

E_{Uv} =   ultrasonic eddy viscosity

E_D =   eddy diffusion coefficient

A Reynolds number for the ultrasonic system can also be developed by using the induced sound velocity, c, from Equation C 38 (Appendix C).

$$\text{Re} = \frac{cD}{k_v}$$ (4 1.2)

Where,

Re =   Reynolds Number

c =   induced sound velocity

D =   characteristic length

40

$$k_v \quad = \quad \text{Kinematic viscosity, cm}^2/\text{s.}$$

The Sherwood Number is a ratio of the mass transfer velocity and the molecular diffusion velocity and can be expressed as a function of the Reynolds Number and the Schmidt Number [28]. Furthermore, the Sherwood Number is a proportional to the mass transfer coefficient.

$$Sh \propto Re^{\alpha} Sc^{\beta} \qquad (4.1\ 3)$$

Where,

Sh =   Sherwood Number

Re^{α} =   Reynolds number

Sc^{β} =   Schmidt number

With the derived Sherwood relationship the qualitative effect of varying the frequency can be approximated to show that the mass transfer coefficient will increase linearly with increasing frequency as detailed in Appendix C

However, when the cavitation pressure is achieved the mass transfer coefficient would be expected to deviate from this relation. Along with the assumption that cavitation would increase the contaminant removal rate, the mass transfer coefficient would be expected to increase substantially

Although the limitations of the experimental equipment prevented validation of this theory, because the frequency and amplitude could not be varied, the data do show that

ultrasonic energy has a large effect on the mass transfer rates. The lack of experimental data provides excellent opportunity for future studies but the available ultrasonics was so effective for this application that there was no programmatic justification for more extensive studies

4.2   BATCH ION EXCHANGE MODEL

4.2.1   Batch Ion Exchange System

The design equation for a constant volume batch system begins with a general mass balance

$$\begin{bmatrix} \text{mass of A} \\ \text{adsorbed} \end{bmatrix} = \begin{bmatrix} \text{mass of A} \\ \text{fed} \end{bmatrix} \bullet \begin{bmatrix} \dfrac{\text{mass of A adsorbed}}{\text{mass of A fed}} \end{bmatrix}$$

$$\begin{bmatrix} \text{mass of A} \\ \text{adsorbed} \end{bmatrix} = [C_{A0}] \quad \bullet \quad [X]$$

The mass of A that remains in the batch reactor after time t, can be expressed in terms of C_{A0} and X

$$\begin{bmatrix} \text{mass of A} \\ \text{in reactor} \\ \text{at time t} \end{bmatrix} = \begin{bmatrix} \text{mass of A} \\ \text{initially fed} \\ \text{to reactor at} \\ t = 0 \end{bmatrix} - \begin{bmatrix} \text{mass of A} \\ \text{that has been} \\ \text{adsorbed onto} \\ \text{ion exchange resin} \end{bmatrix}$$

$$[C_A] \quad = \quad [C_{A0}] \quad - \quad [C_{A0}X]$$

Therefore, the mass of *A* adsorbed onto the ion exchange resin can be expressed by.

$$C_A = C_{Ao} - C_{Ao}X = C_{A0}(1-X)$$
(4 2 1)

Where X relates the mass of A adsorbed to the mass of A fed. This relationship for the adsorption is given by the following ratio

$$X = \frac{mass\,A\,adsorbed}{mass\,of\,A\,fed}$$
(4 2 2)

The mass of A at time t can be expressed in the following differential form

$$\frac{d(C_A V_l)}{dt} = r_A$$
(4 2 3)

For constant volume V_l, integration of Equation 4 2 3 leads to the solution for the time, t, of adsorption of species A onto the ion exchange resin, which is given by

$$t = V_l \int_{C_{A0}}^{C_A} \frac{dC_A}{r_A}$$
(4 2 4)

For the solutes generated from the remediation of the borosilicate Raschig rings, the system was modeled as adsorption or exchange of a single thorium-nitrate complex with a nitrate ion This assumption was made on the basis of the relative concentration

43

differences of thorium to the other species in solution, $C_{Th} \gg \sum C_{All\ Solutes \atop Except\ Th}$ (Table 3 1)   In

addition, the excess ion exchange resin used for the adsorption phase and the higher

affinity of the thorium complex for the adsorption sites relative to the other species

provides a basis for a simplified model

The isotherm for adsorption of species A in a nitric acid system is given by

$$A^- + RNO_3 \leftrightarrow R \bullet A + NO_3^-$$ (4.2 5)

Thorium, as the dominant species, exists in many ionic forms, however, a direct reference

to the various ionic forms was not found but the background information that was

identified provided sufficient information for the separation to be successful [26,27]   The

net rate of adsorption is equal to the rate of molecular attachment to the ion exchange

resin sites minus the rate of detachment over a given surface area, which is also equal to

the concentration change in the bulk fluid medium and is given by [29]

$$r_A = \frac{d}{dt}(C_A) = K_f A_s W_s (C_A - C_A^*)$$ (4 2 6)

where K_f is the overall mass transfer coefficient and A_s is the surface area of the resin

If the loading on the ion exchange resin is small with respect to the mass of the ion

exchange resin and the loading is essentially complete, then C_A^* is in effect zero

From Equation 4 2 3, the rate of adsorption can be shown as

$$\frac{dC_A}{dt} = \frac{K_f A_s W_s}{V_l} C_A$$

(4 2 7)

Equation 4 2 8 can be integrated to yield,

$$\int_{C_{A0}}^{C_A} \frac{dC_A}{C_A} = \int_0^t \frac{K_f A_s W_s}{V_l} dt$$

(4 2 8)

with the initial conditions that when $t = 0$, then $C_A = C_{A0}$ Equation 4 2 10 yields,

$$ln\frac{C_{A0}}{C_A} = kt$$

(4 2 9)

where k is an effective mass transfer coefficient that combines the effect of the surface area of the ion exchange resin, the volume of the liquid, the weight of the species, and the film mass transfer coefficient

The concentration of species A at any time in solution can be determined by taking the natural log of both sides and solving for C_A

$$C_A = C_{A0}\, e^{-kt}$$

(4 2 10)

45

In determining the overall mass transfer coefficient, a relationship can be expressed between the film mass transfer coefficient, k_f, and the solid mass transfer coefficient, k_s

$$\frac{1}{K_f} = \frac{1}{k_f} + \frac{r_p^2}{15 K_d D_A} \qquad (4.2\ 11)$$

where k_f is the film mass transfer coefficient and is given by

$$\frac{1}{k_f} = \frac{D_A(1-\varepsilon)}{v^2 \varepsilon} + \frac{r_p}{3k} \qquad (4.2.12)$$

The solid mass transfer coefficient can be predicted for spherical particles by using the apparent diffusivity of the solute through the solid particles by the following [29]:

$$k_s = \frac{15 D_A}{r_p^2} \qquad (4\ 2\ 13)$$

These relationships provide a means to estimate the mass transfer coefficients and evaluate the effects of variations in resin concentration Fundamentally, this approach was applied in determining the optimum resin concentration for rapid adsorption of the thorium in the batch process as shown in Figure 3 10.   However, extensive experimentation on the effects of the mass transfer coefficient was not performed as the objective of the project was obtained.

5. ECONOMIC ANALYSIS

Cost comparisons for (1) an industrial scale nitric acid/ultrasonic Raschig ring remediation system, (2) an industrial scale surfactant/ultrasonic Raschig ring remediation system, and (3) an alternative treatment process using an existing high-level radioactive waste plant were made by calculating the "future costs" of each plant based on a plant life of five years [30]   During that time, the mobile unit could treat ~35,000 ft^3 of Raschig ring waste   The cost estimates are based on mobile treatment systems that would eliminate the requirements for significant facility site preparation. Costs of post treatment of waste generated were estimated in the disposal costs   The inflation rate was assumed to be at 5% per year   However, it should be noted that these cost estimates are preliminary approximations and should be used only for comparison purposes with other alternatives.

5.1   DESIGN BASES

The following tables provide the design bases for the ultrasonic/nitric acid Raschig ring remediation process and the ultrasonic/surfactant Raschig ring remediation process

Table 5.1 Ultrasonic/Nitric Acid Process System Design Bases

Bases	Specification	Base Estimate
Unit Type	Mobile Unit	
Unit Life	5 – years	
Processed Waste Volume	7,000 ft³/yr (1,000 drums/yr)	
Operation Inflation rate	5%	
Interest rate	12%	
Equipment		
Ultrasonic Tank	100 gallons	$250,000
Filters, Piping, & Installation	2 – 5 micron filters	$385,000
Ion Exchange Column	0.3 m³	$250,000
Secondary Waste & Storage Tanks	2 – 500 gallons	$20,000
Exhaust Fan	800 ft³/hr	$150,000
Virgin Feed Materials		
Nitric Acid	300 lb/yr	
NaOH	500 gal/yr	
Ion Exchange Resin	20 ft³/yr	
Waste Streams		
Drums	1,000 low level radioactive waste	Not costed
Liquid Waste	2,000 gallons/yr	$250,000
Resin	20 ft³/yr	$10,000
Raschig Rings & Sludge	4,000 ft³/yr	$800,000
Services		
Utilities	Electrical, water	$50,000
Maintenance		$115,000
Analytical	Per waste acceptance criteria	$800,000
Labor	Per Appendix D	

Table 5.2 Ultrasonic/Surfactant Process System Design Bases

Bases	Specification	Base Estimate
Unit	Mobile Unit	
Plant Life	5 – years	
Processed Waste Volume	7,000 ft^3/yr (1,000 drums/yr)	
Operation Inflation rate	5%	
Interest rate	12%	
Equipment		
Ultrasonic Tank	100 gallons	$250,000
Piping & Installation		$287,500
Pulverizer	Crush Raschig rings	$175,000
Exhaust Fan	800 ft^3/hr	$150,000
Virgin Feed Materials		
Surfactant	1,000 gal/yr	$4,000
Waste Streams		
Drums	1,000 low level radioactive waste	Not costed.
Salt Cake	4,300 ft3/yr	$758,500
Raschig Rings	2,800 ft^3/yr	$140,000
Services		
Utilities	Electrical, water	$50,000
Analytical	Per waste acceptance criteria	$800,000
Labor	Per Appendix D	

5.2 COST ESTIMATE FOR INDUSTRIAL SCALE ULTRASONIC/NITRIC ACID RASCHIG RING REMEDIATION PROCESS

An industrial scale Raschig ring remediation process would need to be mobile to allow ease of site location near the source of the contaminated Raschig rings. This would reduce the total shipment costs, facility installation costs, and site impact costs The variation in contaminants from site to site would probably result in variations in the process flow diagram to optimize the process Therefore, the final process flow diagram

should be based on nominal sizes to meet the design parameters of a mobile system (i.e.,
trailer or vehicle size).

For the proposed nitric acid/ultrasonic treatment system, scale-up to a bench-top
or pilot design would likely require an ion exchange column, as shown in Figure 5.1.
Preliminary design and experimentation was developed for such a system However in the
laboratory studies, a large pressure drop across the ion exchange column resulted in an
excessive amount of time to perform the separations. The time to perform the column ion
exchange separation in the laboratory resulted in an excessive radiological exposure to the
operations personnel The combination of these two difficulties led to the development of
the batch ion exchange separations. The batch separations could be performed more
safely without continuous observation of the experiment; therefore, reducing radiological
exposure to the operations personnel.

The large pressure drop associated with the laboratory column ion exchange
studies was the result of undissolved contaminants in the solution The same difficulties
were encountered with a fluidized bed ion exchange column design developed at a bench-
top scale Project completion prevented further development of the ion exchange column,
however, this did lead to the design requirements for a filtration unit in the pilot-scale unit
Experience has shown that the amount of undissolved particulate in solution is expected to
be high for remediation of the Raschig rings Therefore, the filtration unit will require a
simple mechanism to minimize the time for cleaning or replacement of the filter element to
satisfy the design requirement of minimizing radiological exposure to the operator
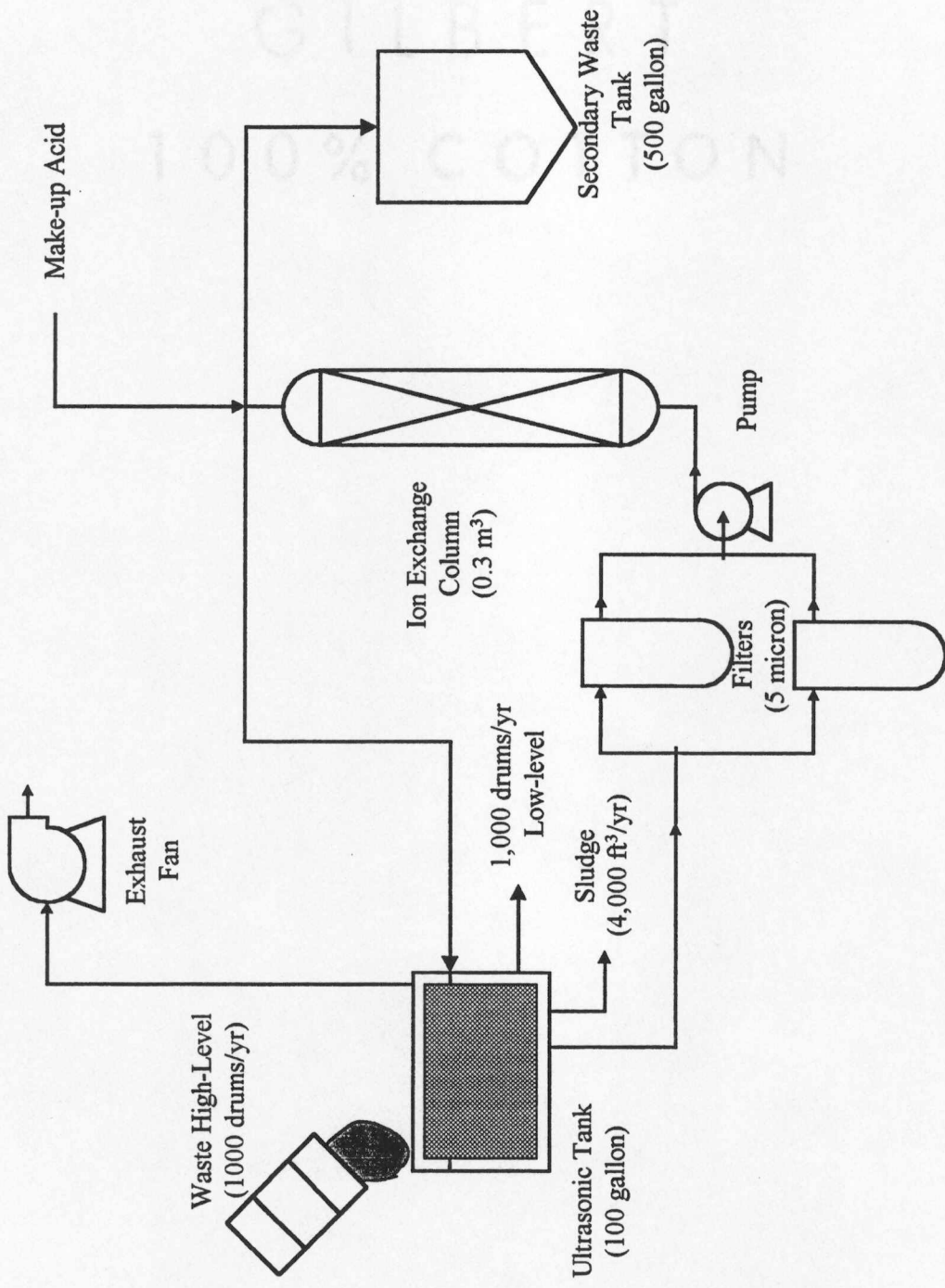
Figure 5.1 Nitric Acid/Ultrasonic Raschig Remediation Industrial Process System

An ion exchange column design was chosen for economic analysis as a standard industrial method; however, the data from the research support a batch design and additional information would be necessary to accurately design a continuous flow column. The actual pros and cons of a column versus batch ion exchange system are better addressed as a function of the waste to be treated.

Disposal costs were derived from estimates used for disposal of low-level radioactive waste at Envirocare of Utah, Inc [31]. Estimates for disposal of expended ion exchange resin were derived from waste acceptance criteria at a local Oak Ridge, TN licensed radioactive waste treatment facility (Scientific Ecology Group, Inc.) [32]. Labor costs were determined at a fully burdened rate of $100/hr (Appendix D). Table 5 3 contains overall cost estimates for an industrial scale nitric acid/ultrasonic Raschig ring remediation system.

5.3 COST ESTIMATE FOR ULTRASONIC/SURFACTANT RASCHIG RING REMEDIATION PROCESS

A process flow diagram of the proposed surfactant/ultrasonic remediation process is shown in Figure 5.2 The proposed system is a batch design, which simplifies the operation The secondary waste generated is limited to the contaminated salt cake A basis was assumed to process one thousand drums of Raschig rings per year. A conservative contaminated sludge volume of 0.0012 ft^3/ring was estimated by assuming the center of the Raschig ring was filled with sludge and an approximately 1/8" layer coated the exterior of the Raschig ring This was approximately twice the thickness of the sludge encountered during the remediation studies of this project This combined

Table 5.3   Cost Estimate for Industrial Scale Nitric Acid/Ultrasonic Raschig Ring Remediation Process.

CATEGORY	$/year 1	$/year 2[1]
Operating Costs		
Labor[2]	1,400,000	
Chemicals		
Nitric Acid (300 lb/yr @ $0 85/lb)	255	
NaOH (500 gal/yr @ $1.30/gal)	650	
Ion Exchange Materials		
Reillex HPQ resin (~ 20 ft³/yr @ $100/ft³)	2,000	
Utilities	50,000	
Maintenance	115,000	
Analytical Services	800,000	____
Total + 10% contingency	2,604,696	2,734,930
Capital Costs[3]		
Ion Exchange Column (~ 0.3 m³ skid mounted)	350,000	
Ultrasonic Tank with instrumentation and controls	250,000	
Storage Tanks	20,000	
Exhaust Ventilation System	150,000	
Installation Costs (includes piping and trailer)	385,000	____
Total + 10% contingency	1,270,500	-
Disposal Costs		
Liquid Wastes (Dilute 2,000 gal/yr @ $125/gal)	250,000	
Solid Wastes (Raschig rings @ $50/ft³, Sludge @ $200/ft³)	800,000	
Ion Exchange Resin (20 ft³/yr @ $500/ft³)	10,000	____
Total + 10% contingency	1,166,000	1,224,300

Note 1 Costs for years 3 - 5 can be estimated by applying a 5% escalation
Note 2. Labor costs are detailed in Appendix D.
Note 3 Capitalization costs were estimated at 12% interest per Appendix D

Exhaust Fan

Salt Cake
(4,300 ft³/yr)

Waste
(1,000 drums/yr)

Surfactant
(1000 gal/yr)

Ultrasonic Sink
(100 gallon tank)

Pulverizer

Pulverized Raschig Rings
(377 drums/yr)

Figure 5.2 Surfactant/Ultrasonic Raschig Ring Remediation Industrial Process

54

with a 20% estimate of solutes in the surfactant results in a volume estimate of ~4,300 ft³/yr of salt cake   An additional pulverization operation is added to reduce the volume of the Raschig rings   This results in approximately a 60% reduction in volume of the Raschig rings   Cost estimates for the surfactant/ultrasonic Raschig ring remediation process are given in Table 5 4

5.4 ALTERNATIVE PROCESS TO REMEDIATION OF BOROSILICATE RASCHIG RINGS

For project completeness, an alternative process is discussed for disposal/treatment of radioactively contaminated Raschig rings   Currently, there is in operation a high-level radioactive vitrification process at the U.S. Department of Energy Savannah River Plant (SRP) in Aiken, South Carolina   The process is based on high temperature treatment of high-level waste while glass formers are added to the waste stream to produce a solidified glass matrix that encapsulates and bonds the radioactive contaminates   Borosilicate glass has been selected as the optimum choice for the glass matrix feedstock [33]   Therefore, it is apparent that after proper sizing the radioactive borosilicate Raschig rings could be blended into the glass former feed   Furthermore, the process is in operation, the disposal/treatment costs of the Raschig rings would only be incremental and not fully burdened by the outlay of costs presented in the previous processes

Table 5.4   Cost Estimate for Industrial Scale Surfactant/Ultrasonic Raschig Ring Remediation Process.

CATEGORY	$/year	$/year[1]
Operating Costs		
Labor (20% reduction for simpler process)[2]	1,120,000	
Chemicals		
Surfactant (1000 gal/yr @ $4 00/gal)	4,000	
Utilities	50,000	
Analytical Services	800,000	_____
Total + 10% contingency	2,171,400	2,279,970
Capital Costs[3]		
Ultrasonic Tank with instrumentation and controls	250,000	
Pulverizer	175,000	
Exhaust Ventilation/Off-Gas Treatment System	150,000	
Installation Costs (includes piping and trailer)	287,500	_____
Total + 10% contingency	948,750	-
Disposal Costs		
Liquid Wastes (no secondary liquid waste generated)		
Solid Wastes		
(salt cake @ $~175/ft^3, Raschig rings @ $50/ft^3)	898,500	_____
Total + 10% contingency	988,350	1,037,768

Note 1 Costs for years 3 - 5 can be estimated by applying a 5% escalation
Note 2 Labor costs are detailed in Appendix D
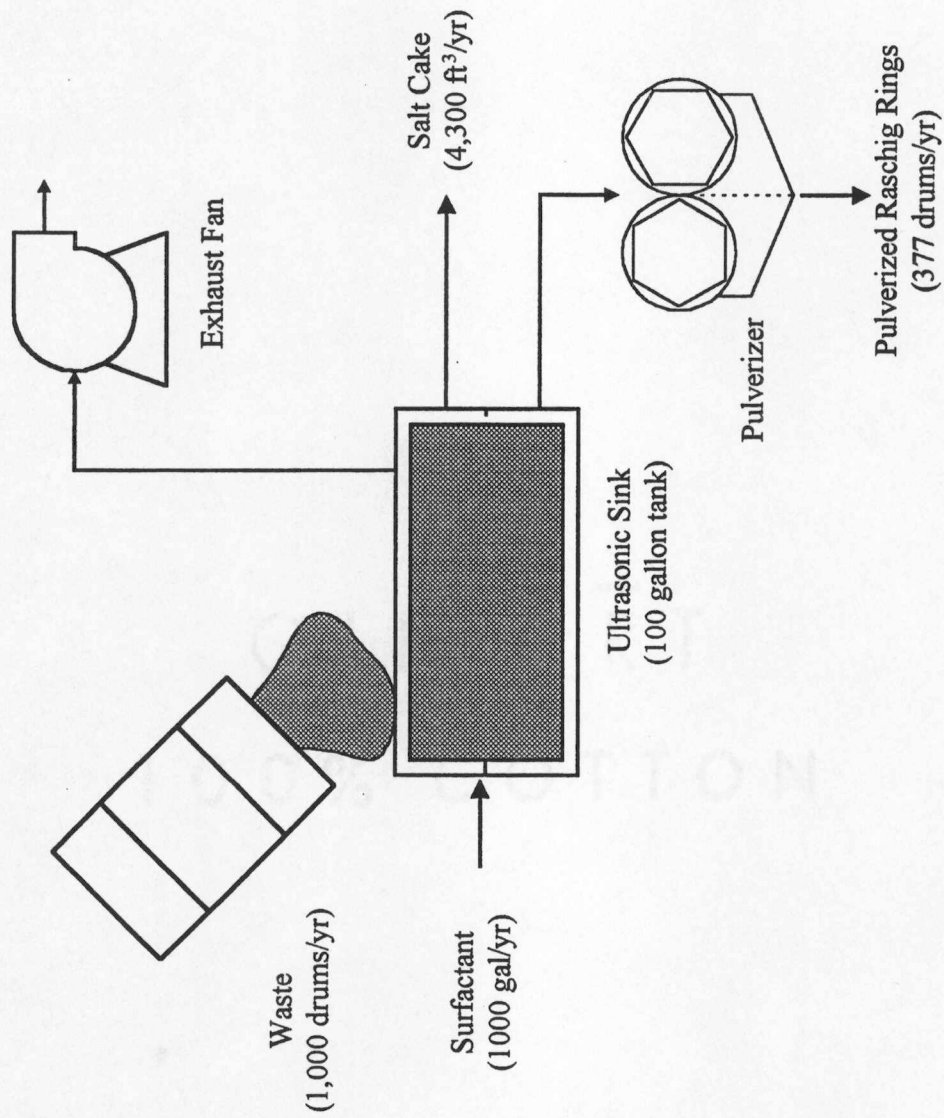Note 3 Capitalization costs were estimated at 12% interest per Appendix D.

Insufficient information was available to determine the incremental costs However, an assumption was made for a capital modification of ~$250K to provide grinding equipment to prepare the borosilicate Raschig rings for appropriate feedstock The labor could also be substantially reduced to an incremental cost of ~25% or one full time equivalent ($280K) of the surfactant/ultrasonic process Additional costs associated with the SRP option include the potential costs of packaging and shipping the wastes and expenses from SRP to receive and treat the wastes Since these costs involve SRP policies and depend upon costs to change the large existing facility operations, an accurate assessment of costs for this option is beyond the scope of this study but the option is mentioned here for completeness of other potential alternatives

The designs for ultrasonic remediation processes provide a basis from which to determine the overall potential cost savings of using the existing vitrification process at SRP. In addition, for waste streams that are not acceptable at the SRP the ultrasonic remediation processes provide an alternative for mobile treatment and volume reduction of highly contaminated Raschig ring waste streams

5.5 COST COMPARISON OF PROPOSED RASCHIG RING REMEDIATION SYSTEMS

Cost comparisons of the nitric acid/ultrasonic system versus the surfactant/ultrasonic system are summarized in Table 5.5 The systems were compared on the basis of yearly operating costs, capital investment costs, and yearly disposal costs The future value of the initial capital investment costs were determined over a five year

Table 5.5   Cost estimate comparison of Nitric Acid/Ultrasonic System to Surfactant/Ultrasonic system.

Cost Summary

$/year 1

	Nitric Acid/Ultrasonic System	Surfactant/Ultrasonic System
Capital Costs	1,270,500	948,750
Operating Costs/yr	2,604,696	2,171,400
Disposal Costs/yr	1,166,000	988,350
Total Yearly Costs	5,041,196	4,108,500

Future Value Costs

$/year 5

	Nitric Acid/Ultrasonic System	Surfactant/Ultrasonic System
5-Year Operating and Disposal Costs (5% Inflation/yr + 10% contingency)	20,835,476	17,459,613
5-Year Future Capital Costs at Startup in 2000	1,631,354	1,218,219
Total Value Capital Costs Plus Disposal Costs ($/year 5)	22,477,741	18,644,618

Table 5.5 (continued)

	Cost Savings (5 year basis)		
		No Remediation of Raschig Rings	
	Nitric Acid/ Ultrasonic System	Low-level Radioactive Waste	Transuranic Radioactive Waste
Surfactant/Ultrasonics Versus Alternatives	3,833,000	(17,769,000)	7,605,000

expected operating life of the project. No credit for depreciation recovery costs or salvage value was taken at the end of the project life due to the probability that the equipment would be radioactively contaminated and become a liability for disposal. Furthermore, an assumption was made that the decontamination and demolition costs would be equivalent for each system   A summary for the formulas used in the economic analysis is given in Appendix D

Results of the cost comparison of the surfactant/ultrasonic system over the nitric acid/ultrasonic system show relative savings of over $2 9M for a five-year period.   The cost comparison is obtained when comparing the capital, operating, and disposal costs to the two types of radioactive wastes (low-level and transuranic). Additional benefits are obtained from the surfactant/ultrasonic from the integral use of a safer solvent and simpler design. The results show no savings for processing low-level radioactive waste; however, substantial savings are obtainable by processing transuranic waste   An additional alternative, as with this project, is the potential recovery of a product (i e., thorium-229) from the waste that could offset the costs of processing

6. CONCLUSIONS AND RECOMMENDATIONS

This study has successfully demonstrated its primary objective to remediate radioactively contaminated borosilicate Raschig rings Two relatively simple methods of remediation were developed that achieved greater than 99% removal of the radioactive contaminants, which is below the current transuranic regulatory limit of 100 nCi/g (5 8 μCi/Raschig ring). The first utilized a combination of nitric acid/ultrasonics and ion exchange processes. The radioactive contaminants were removed from the Raschig rings with nitric acid/ultrasonics, and the contaminants were recovered via ion exchange.

An alternative process was developed for economic and operational comparison The process utilized a combination of surfactant and ultrasonic agitation to remove the contaminants The surfactant was then evaporated, to demonstrate volume reduction, to form a salt cake, which provided a concentrated solid for disposal

Both remediation methods were developed on a laboratory scale for a single radioactive waste stream Therefore, the results should be applicable to other similar waste streams and could be used to provide data for scale-up of processes to a bench-top or small pilot plant level

The success of this project is linked directly to the effects of the ultrasonic agitation From the experimental data, a direct correlation was made to the effects of ultrasonics to account for the rapid success of the project at remediating the radioactively contaminated Raschig rings Basic mass transfer theory was applied to the ultrasonic

cavitation system in an effort provide insight into the mechanism of ultrasonic enhancements. Follow on research, where the frequency and power can be controlled, would be necessary to validate the proposed relationships between ultrasonic eddy diffusion and the mass transfer model

Results from the laboratory studies established fundamental data to support design of an effective remediation process In addition, the potential economic savings from the remediation of contaminated Raschig rings and the volume reduction of transuranic wastes were shown to justify further investigation into remediation of this type of waste stream. Application of a mobile remediation unit would be exceptionally attractive for locations with limited space and at dispersed sites that contain Raschig rings.

From the economic evaluation, the surfactant/ultrasonic remediation unit offers significant advantages over the nitric acid/ultrasonic unit The surfactant/ultrasonic system was estimated to be less expensive to operate, construct, and dispose of secondary waste streams. The batch nature of the operation offers a simpler system for operation and maintenance. Furthermore, the fewer major components result in a reduced space requirement Therefore, this system would be easier to mobilize from site to site. Overall, the surfactant/ultrasonic system is safer to operate, more economical to construct, produces fewer secondary wastes, and can meet the radiological design intent for low exposure to personnel

The secondary objective to recover thorium-229 from the Raschig rings was successful through ion exchange separation with anion and cation type resins The

successful recovery of the thorium-229 provided the material to continue to support the research and development of alpha radioimmunotherapy

The experimental provides the basis to continue in both directions of research 1) the theory of the mass transfer mechanisms of the ultrasonic cavitation system and 2) development of a bench-scale remediation system.

REFERENCES

REFERENCES

1. J P Nichols, C L Shuske, D. W Magnuson, Use of Borosilicate-Glass Raschig Rings as a Neutron Absorber in Solutions of Fissile Material, *Y-CDC-9*, Union Carbide Corporation, Oak Ridge Y-12 Plant, July 1971

2. ANSI/ANS 1986, Use of Borosilicate-Glass Raschig Rings as a Neutron Absorber in Solutions of Fissile Materials, ANSI/ANS-8 5-1986, American Nuclear Society, La Grange Park, Illinois.

3. ANSI/ANS 1994, Use of Borosilicate-Glass Raschig Rings as a Neutron Absorber in Solutions of Fissile Materials, ANSI/ANS 8.5 Standard Revision 94-2 ANSI/ANS-8.5-1994, American Nuclear Society, Standards Committee, Working Group ANS-8.5., La Grange Park, Illinois

4. Quote supplied by First Choice Technical Services, Inc for U.S. Department of Energy radioactive waste disposal costs, Tom Price, May 1998

5. K R. Givens, *Separation Science and Technology*, 32, 405,1997.

6. S M Larson, *J. Nuclear Medicine*, 26, 538, 1985.

7. R. M. Macklis, et al , *Int. J. Radiation Oncology Biol. Phys.*, 16, 1377, 1988

8. A. N. Houghton and D. A Shienberg, *Seminars in Oncology*, 13, 165, 1986.

9. R M Macklis, et al , *Radiation Research*, 130, 220, 1992.

10. J Broothaerts, et al , Industrial Experience Gained In the Decontamination of Process Cells, the Dismantling of Process Equipment, and the Conditioning of Special Solid Wastes in a Shut-Down Reprocessing Plant, Proceedings of an

International Symposium on the Decommissioning of Nuclear Facilities, Vienna, November 13-17, 1978.

11.   EG&G Rocky Flats, Inc , "Raschig Ring Trade Study", March 1995

12   Information supplied by Judy Butler, Facility Supervisor, Oak Ridge National Laboratory, April, 1995

13   J J Cohen, C. F Smith, and F. J. Ciminese, "Nuclear Waste Issues - A Perspectives Document", UCRL-15530, Lawrence Livermore Laboratory, Livermore, CA (1983)

14.   D. E Gordon and T A. Bernadzikowski, "National Program for Immobilization of High-Level Radioactive Wastes", presented at the Second Joint ASME/ANS Nuclear Engineering Conference, American Society of Mechanical Engineers Paper 82-NE-34 (1982)

15   Oak Ridge National Laboratory, Radiochemical Analytical Laboratory, Analytical Notes via telecommunication, November 1994.

16   Oak Ridge National Laboratory, Radiochemical Analytical Laboratory, Analytical Laboratory Results, September 1994.

17   "Standard Practice for Designing a Process for Cleaning Technical Glasses," ASTM C 912, 1985 Annual Book of ASTM Standards, Section 15, Vol. 15.02, American Society for Testing and Materials, Philadelphia, pp 538-546

18   Pantano, C G., Jr. and Hench, L.L , "Cleaning Borosilicate Glass for Biological Applications," *Journal of Testing and Evaluation*, 5, 1977, pp 66-69

19   Harding, W.B., "Evaluation of Surfactant-Water Mixtures as Cleaning Agents," *KCP-613-5001*, 1993

20. Slanina, J. T , "Conversion from Solvent to Aqueous Chemistries for the Final Cleaning of Printed Wiring Boards in a Printed Wiring Board Facility," *KCP-613-4654*, 1992

21. Gollapudi, U K., et al., "Ultrasonic Treatment of Removal of Asphaltene Deposits During Petroleum Production," *SPE International Symposium on Formation Damage Control*, 1994.

22. Knolls, J. R., "Flat Glass Washing – Techniques and Compounds," *Glass*, 1989, <u>66</u>, 19

23. U. S Department of Energy, "Radioactive Waste Management", U. S DOE Order 5820.2A, September 1988

24. U.S Nuclear Waste Policy Act of 1982

25. U S. Code of Federal Regulations Title 40, Part 191

26. R H Rainey, "Laboratory Development of a Pressurized Cation Exchange Process for Removing the Daughters of ^{232}U from ^{233}U", *ORNL-4731*, December 1972.

27. D. C Overholt, "An Ion-Exchange Process for ^{233}U Isolation and Purification", *ORNL-1364*, September 1952

28. Sherwood, T K , Pigford, R L , and Pigford, C R., <u>Mass Transfer</u>, McGraw Hill, New York, 1975

29. Watson, Jack S , <u>Separation Methods for Waste and Environmental Applications</u>, Marcel Dekker, Inc , New York, 1999.

30. Peters, M. S., and Timmerhaus, K. D , Plant Design and Economics for Chemical Engineers, 4th ed., McGraw Hill, New York, 1980

31 Quote supplied by First Choice Technical Services, Inc. for U.S Department of Energy low-level disposal costs, Tom Price, May 1998

32 Quote supplied by Molten Metal Technology, Inc. for solidification and/or disposal of low-level radioactive resin, Mathew Howell, August, 1996.

33. Wicks and D F. Bickford, "High Level Radioactive Waste - Doing Something About It," *DP-1777*, March 1989.

34 G.G. Stokes, Trans Camb. Phil. Soc., 1849, 8, 287

35 G. Kirchoff, Ann Phys (Leipzig), 1868, 134, 177

36 T.J. Mason and J P. Lorimer, Sonochemistry, Theory, Applications and Uses of Ultrasound in Chemistry, John Wiley and Sons, New York, 1988.

37 D. H Trevena, Cavitation and Tension in Liquids, 1987, IOP Publishing Ltd..

38. Jasper, J.J , J. Phys. Chem Ref. Data, 1989, 1, 841.

39 R C Reid, J.M Prausnitz, and B E Poling, The Properties of Gases & Liquids, McGraw Hill, New York, 1987

40. R B. Bird, W. E. Stewart, and E N Lightfoot, Transport Phenomena, John Wiley and Sons, New York, 1960

41. B Carlin, Ultrasonics, McGraw Hill, New York, 1960.

42 J F Fuchs, "Ultrasonic Cleaning," *Metal Finishing*, 90, No 1A, 139-144, January 1993

43.   Qi, Q and G. J. Brereton, *IEEE Transactions on Ultrasonics, Ferroelectrics, and Frequency Control*, July 1995, <u>4</u>, 42.

44   C.E Harland, <u>Ion Exchange Theory and Practice, 2nd ed</u>, The Royal Society of Chemistry, Cambridge, UK , 1994.

APPENDICES

Appendix A

FUNDAMENTAL THEORY OF GAMMA SPECTROSCOPY

The following citation was obtained from the operation manual of the Canberra SU-450 gamma spectroscopy unit.

GAMMA INTERACTION WITH MATTER

There are three primary mechanisms of interaction of photons with matter. These are the photoelectric effect, Compton scattering, and pair production. The photoelectric effect and Compton scattering involve the interaction of photons with the orbital electrons of the absorber These interactions predominate when the photon energy does not greatly exceed 1.02 MeV, the rest mass energy of two electrons Pair production involves the direct conversion of electromagnetic energy into mass This type of interaction predominates with photons of higher energy. These interaction mechanisms are illustrated in Figure A 1 and described in greater detail in the following sections

Photoelectric Effect

The photoelectric effect occurs when a photon interacts with a tightly bound orbital electron and disappears. The orbital electron is ejected from the atom with a kinetic energy equal to the difference between the incident photon energy and the binding energy of the electron

$$E_{e^-} = E_\gamma - E_b$$

The photoelectric effect is favored by low energy photons and high-atomic numbered absorbers. The probability of this interaction can be approximated by·

$$\frac{Z^4}{E^3} \text{ or } \frac{Z^5}{E^3}$$

71

Where:

Z^4 is for low energy photons

Z^5 is for high energy photons

E^3 in the denominator indicates that this process is predominant for low energy photons

Z term shows enhancement of the process with high Z materials

The relative importance of the photoelectric effect in various absorber materials for

various photon energies is shown in Figure A.2.

Photoelectric Effect
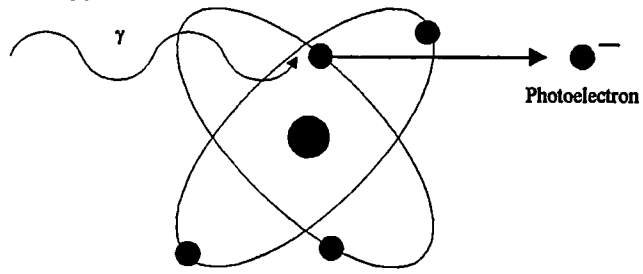
Compton Scattering
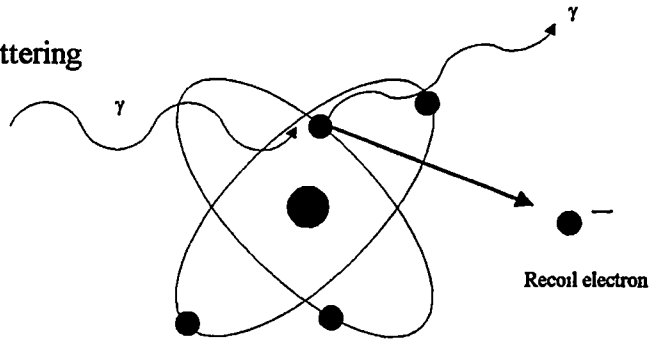
Pair Production
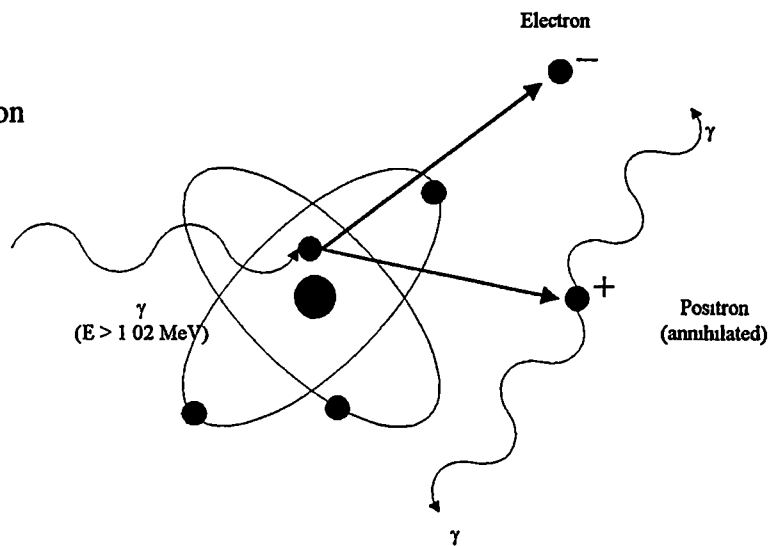
Figure A-1. Mechanism of interaction of photons with matter.

73
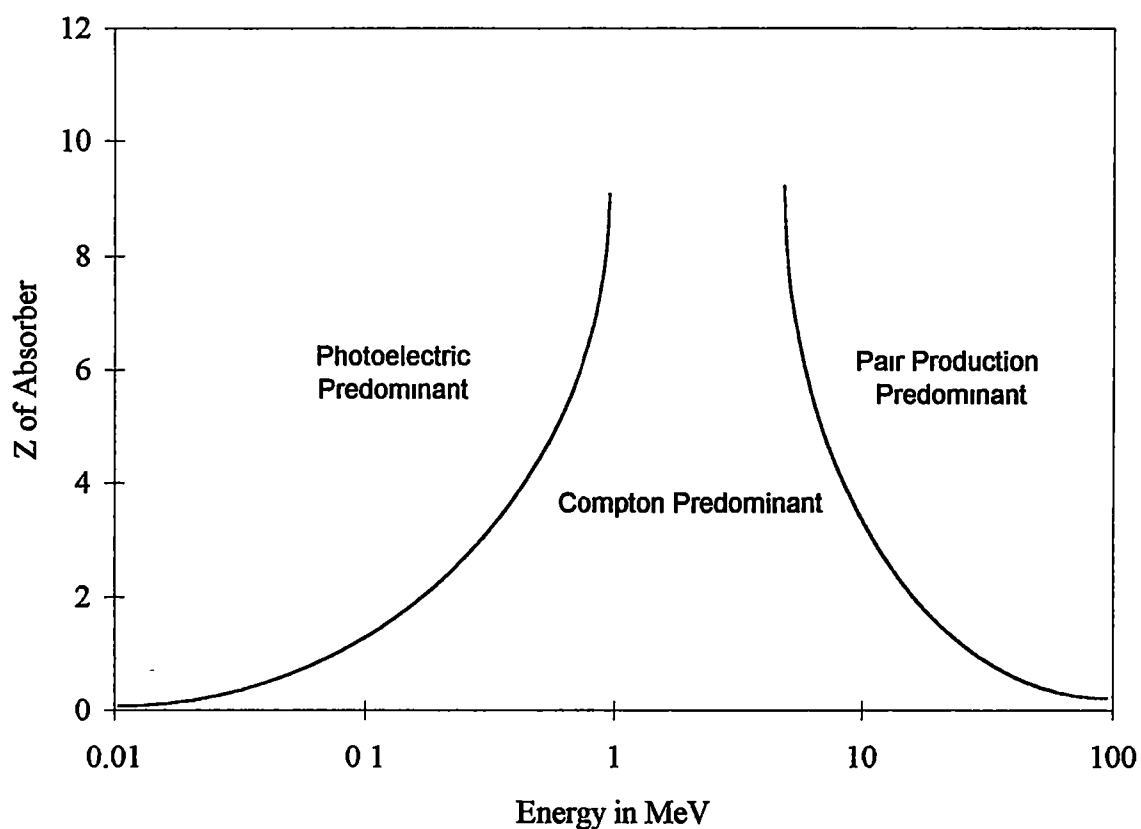
Figure A-2. Probability of photon interactions as a function of different absorber materials and photon energies.

Compton Scattering

Compton scattering is the elastic scattering of a photon by an electron in which both energy and momentum are conserved. As shown in Figure A-1, the incident photon is scattered through an angle and the impacted electron recoils This electron is called the recoil electron. Since the recoiling electron acquires some kinetic energy from this collision, the energy of the scattered photon is less than the incident photon.

The energy of the scattered photon is calculated by the following equation:

$$E'' = \frac{E(0.511\text{MeV})}{0.511\text{MeV} + E(1 - cos\theta)}$$

Where

E" = Energy of scattered gamma

E = Energy of incident gamma

θ = Scattering angle

The 0 511 MeV is the rest-mass energy of the electron. As seen by the equation, the energy of the scattered photon is dependent on the angle of scatter. The probability of a Compton interaction decreases with increasing photon energy and with increasing atomic number. This is illustrated in Figure A.2 Figure A 2 shows that Compton scattering is the dominant mode of interaction from about 0.5 to 5 0 MeV.

Pair Production

A photon whose energy exceeds 1 02 MeV may, as it passes near a nucleus, disappear and its energy reappear as a positron and electron in the process called pair production The 1 02 MeV is the rest-mass energy of two electrons, 2 x 0 511 MeV The total kinetic energy of the positron-electron pair is equal to the energy of the photon minus 1.02 MeV Once formed, the positron and electron move about and lose energy as a result of collisions with atoms in the surrounding medium After the positron has slowed down to a very low energy, it combines with an electron and the two particles disappear They are replaced by two photons each having energy of 0.511 MeV These photons are called

annihilator radiation   As shown in Figure A 2, the probability of pair production increases with increasing energy.

THE SPECTRUM

The number of counts per unit time in a multi-channel analyzer spectrum channel is equal to the number of pulses of a certain height seen by the counting system during the live time   The peak of a monoenergetic gamma ideally would be one channel wide. Detector and system characteristics result in monoenergetic gamma producing pulses of slightly different heights due to counting noise and slight differences in charge collection.

The various features of a spectrum are due to the different interactions or sequences of interactions, which occur in the detector. The probability of a particular spectral feature occurring is related to the probability that a particular interaction (or sequence of interactions) takes place   Figure A.3 shows some spectral features, which may appear in a spectrum as a result of these interactions
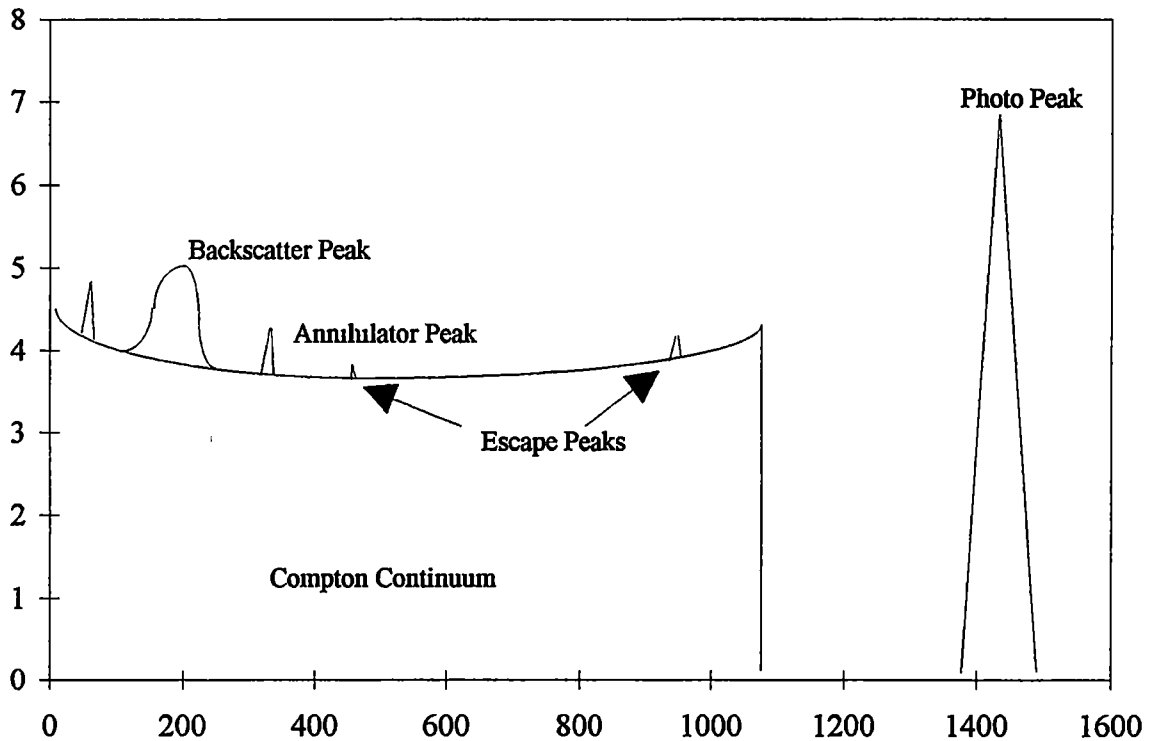
Figure A-3. Spectral characteristics

Typical features found in spectra

1 Photopeak - The peak which results from primary photoelectric interactions and other sequences of interactions which deposit the full energy of a particular gamma-ray into the detector These peaks are used to qualify and quantify the nuclide

2. Backscatter Peak - This peak results from the 180° backscatter during Compton interaction. This peak is typically found between 180 and 250 keV depending on the energy of the incident gamma

3 Compton Edge - This characteristic of the spectrums found at the energy of the photopeak minus the energy of the backscatter peak

4. Annihilation Peak - Found following positron annihilation. The peak is found at 511 keV

5. Multiplets - These are peaks which overlap.

77

6   Compton Continuum - That portion of the spectrum which is produced by the scattered gamma from Compton interaction. The Compton continuum is also referred to as the continuum background The counts, which make up this region are not considered in the calculation of the peak area The number of counts in this area will affect the minimum detectable activity calculated for the particular peak.

7   X-ray Peaks - Certain nuclide have decay schemes, which produce X-rays These are typically low energy These peaks must be used to quantify certain nuclide, such as I-125. Complications can arise during calibrations because of the interference of X-rays from other nuclide.   Special detector caps are required to analyze X-rays properly Also, X-rays are produced by the interaction of the gamma with material in the shielding The 72, 75, and 85 keV fluorescence x-rays of lead are common.

8   Ge Escape Peaks - When photoelectric absorption occurs, the absorber atom emits an x-ray. It is typically reabsorbed with the peak However, if the interactions occur near the surface of the detector, the x-ray may escape. The gamma produced will be the energy of the gamma minus the energy of the x-ray.

9   Environmental Background Peaks - These are photopeaks which are caused by the presence of external contamination on the detector or chair, high activity sources in the area or airborne radioactivity.

10 Single Escape Peaks - These result from the escape of an annihilation photon following a pair production interaction   The energy of the peak is 511 keV less than the photopeak

11 Double Escape Peaks - These result from the escape of both annihilation photons following a pair production interaction. The energy of the peak is 1022 keV less than the photopeak

12 Coincidence-sum peak - These are photo peaks caused by the simultaneous detection of two gamma usually from a single nuclide   These are predominant in well detectors or with extremely high-count rates

ENERGY CALIBRATION

In order to determine the amounts and various types of radionuclide in an unknown sample, calibrations must be performed to provide a base level for analysis. To identify the nuclide or the number of microcurie in the sample, it is necessary to have information

on the energy versus channel relationship of the ADC, in addition to the peak width versus energy relationship of the peaks

The energy calibration provides the following

Energy-Channel Relationship

The amplifier gain and ADC zero adjustments are adjusted to modify the amplitude of the pulses so that the peaks fall into the appropriate channels. These adjustments must be selected so that the peaks of interest will be registered within the available number of channels.

The typical energy calibration, for the 4096 channel Ge spectrum, is 0.5 keV/channel. This is based on a maximum energy of 2000 keV If other maximum energies are appropriate to the application then other gains may be applicable Caution should be taken not to spread out the spectra to a point where the peaks are flattened excessively

Once this general setup is established a source of known energies is collected. The relationship between the centroid of the peaks and the channels in which they appear are plotted A curve is fitted to this line and the energy of any unknown peak can be taken from this curve as illustrated by Figure A 4.
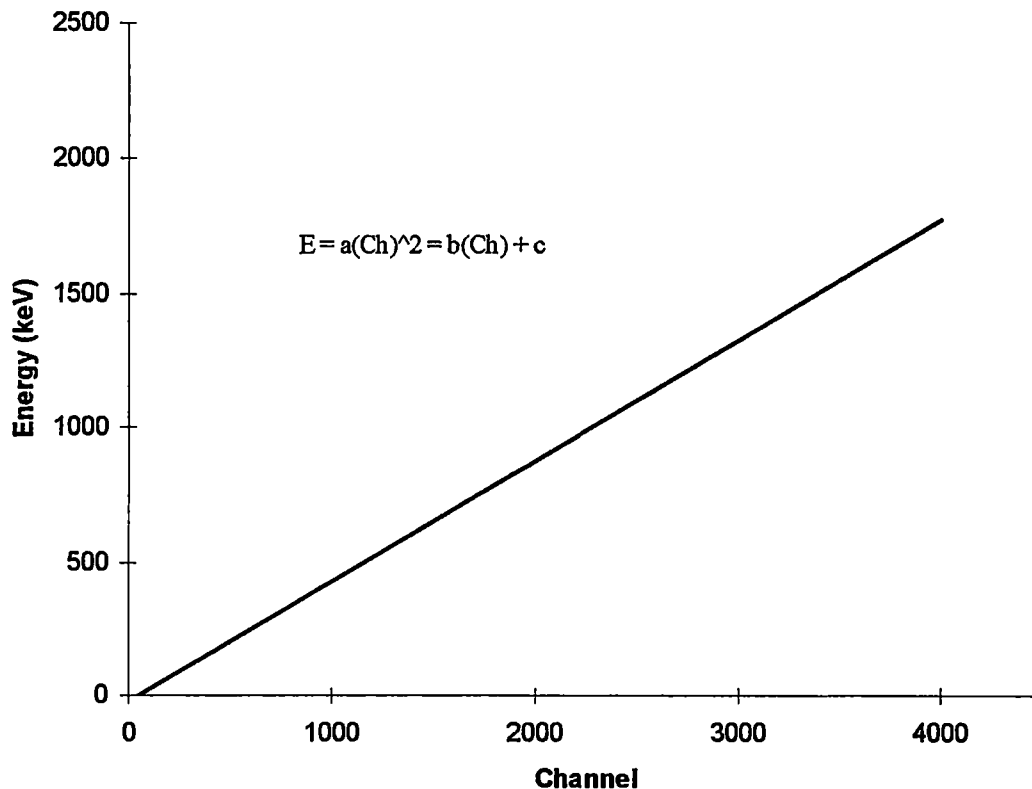
Figure A-4. Energy calibration curve.

To properly energy calibrate an ADC the source used should have the following

properties

1   Energies which span the full range of interest   Due to the slight non-linearity of detector systems, the curve should not be extrapolated past the end-points

2   The source strength should be sufficient to produce statistically significant peaks in a reasonable count time

3   Peaks selected for the calibration should be well-defined singlet peaks.

4   The source should not be placed directly against the face of the detector   At least a few millimeters should be allowed to prevent complication of the spectra

Full Width at Half Maximum

The Full Width at Half Maximum (FWHM) is a measure of the width of the peak at half its maximum height   Figure A 5 illustrates the FWHM and the FWTM (Full Width at Tenth Maximum)   These parameters define the shape of the peak.
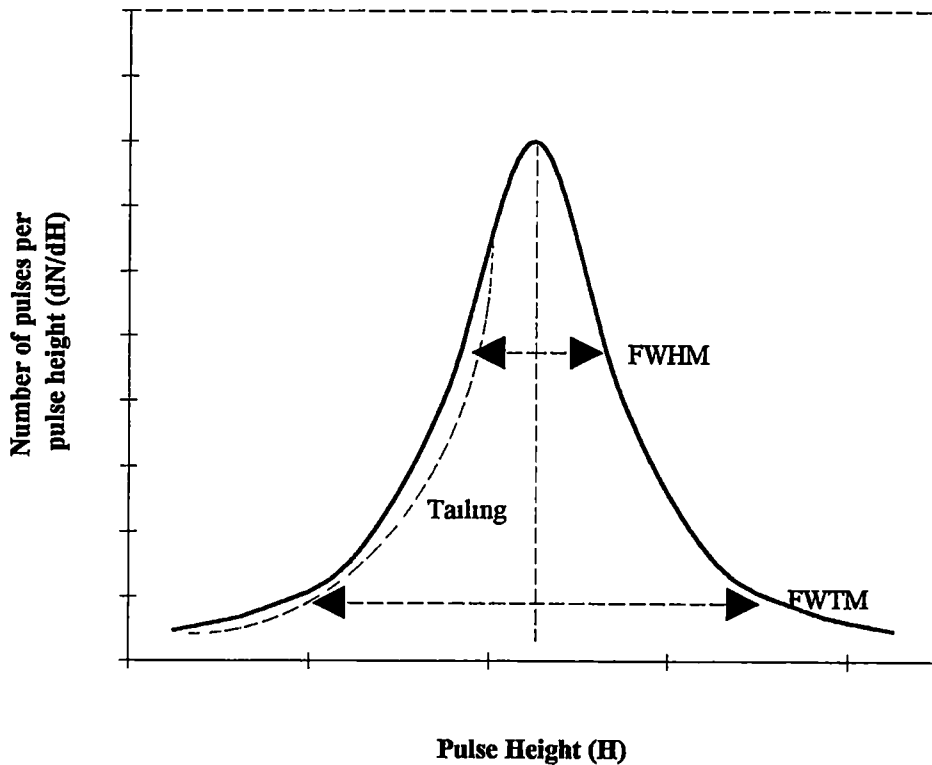
Figure A-5. FWHM, FWTM, and tailing

There are three fundamental causes of peak broadening in the spectrum.

1   Statistical fluctuations in the charge (or number of scintillations) produced from event to event   This is the most significant contributor to the resolution

2. Electronic noise

3   Variations in charge (or light) collection efficiency.

81

In addition to these fundamental contributors, a consideration in the real world is that of instrument drift. If any instrument in the signal chain drifts during the collection of the spectrum, an additional broadening of the observed spectral peak will result. This is especially true during long counts

In spectral analyses, the FWHM is also used to determine if peaks are overlapping When overlapping occurs, the width of peak is used to determine which portion of the total net area should be attributed to each peak. The FWHM increases with increasing gamma energy

The FWHM is also used as a measure of the resolution of a detector. When used for resolution determination, the FWHM is measured under specific conditions, such as, source to detector distance, gamma energy, and intensity Detectors are related on this parameter

FWHM is usually expressed in channels or keV Resolution for germanium detectors is expressed in terms of FWHM. The smaller the FWHM or resolution, the more easily you can distinguish between peaks of similar energies Although the FWHM increases with gamma energy, the resolution becomes better with higher gamma energy Increasing the gain of the detector will typically increase the FWHM The width of the peaks generally increases as the energy of the gamma increases. Then Ge peaks are considered, the tailing, or deviation from the Gaussian shape, is also measured. The tailing on the low energy side of the peak is most prominent and is most often considered

GAMMA SPECTRAL ANALYSIS

Once the spectroscopy system is energy calibrated analysis of spectrum energies can be accomplished   Peak locations can be determined and compared with library energies to determine what radionuclides are present. To determine the quantity, i e. activities, of the nuclide further analysis of the spectral peaks is required.

Calculation of Net Peak Area

It is necessary to determine the net peak area, rather than merely total the counts in each channel   The total integral under a peak represents both counts arising from the full disposition of the energy of the gamma of interest and the random pulses caused by the Compton scatter of higher energy gamma   Peak energy determination can be facilitated be selecting a region of interest where there is obviously a peak   This will temporarily eliminate considerations of minimum detectable activity and multiplets.

Region of Interest

The general shape of the peak is 'Gaussian ' This is a bell shaped curve that is shown in Figure A 6. The peak is determined to begin at the first positive change of slope and end at the second positive change in slope   Obviously, slight differences in the channel heights may cause slight deviation from this

Since the fraction of the peak area at or near the background channel is very small, choosing one channel as opposed to the next will not change the peak area significantly.

This is especially true for well-separated peaks. In Ge spectrum the centroid of a singlet peak is usually obvious. This will be used in determining the FWHM and the energy of the peak.
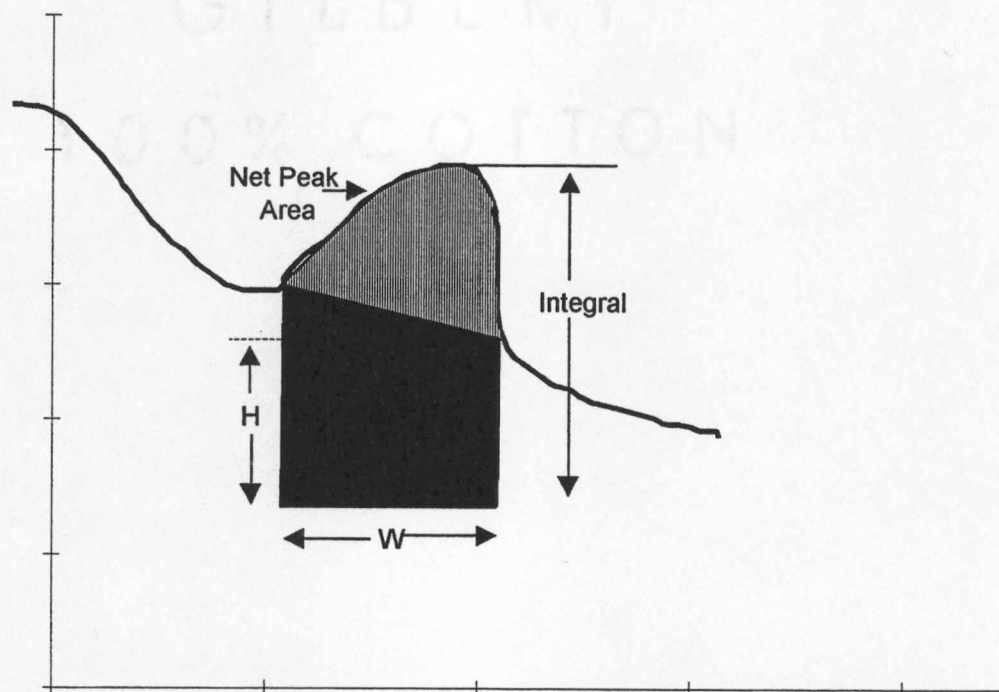
Figure A-6. Determination of net peak area.

Once the region of interest is selected we can determine the background area as follows. The example calculation and the methodology described in Figure A.6 is used here. The background is estimated by finding the average height of the background channels and multiplying it times the number of channels in the peak. The average height is calculated

from the 4 channels immediately preceding and immediately following the peak channels.

The number may vary depending on the proximity of other peaks in the spectrum.

W = Width of background in channels

H = Height of background

The height of the background is calculated by taking 2-4 points on each side of the peak

Example: (Assume 4 points on each side)

$$A_{BKG} = W * H$$
$$= W * \frac{1}{2}(\frac{1}{4}\sum L_{BKG} + \frac{1}{4}\sum R_{BKG})$$
$$= W * \frac{1}{8}(\sum Ch_{BKG})$$

Where

$\sum L_{BKG}$ = total number of background counts in the (4) channels on the left hand side of the peak.

$\sum R_{BKG}$ = total number of background counts in the (4) channels on the right hand side of the peak

Calculate the Net Peak Area

The counts in each channel in the selected region of interest are totaled. This is referred to as the integral   The following equation is used to calculate the net area.

Area = Integral - Background

Determine the Energy of the Peak Centroid

The gamma spectroscopy software or microprocessor of the multi-channel analyzer will produce an equation for the energy/channel relationship similar to the one that follows.

$$Energy\ (keV) = C + B(ch) + A(ch)^2$$

Some software packages may add a cubed term if a sufficient number of peaks were used in the calibration

This equation should be reviewed when the calibration or autocalibration is performed. Each value has limits. Some typical limits are listed below The exact limits for each facility will vary

1. C = the offset This should be close to zero.

2   B = the gain in keV/channel A typical value is 0.5 for germanium systems with 4096 channels of multi-channel analyzer memory.

3. A = the nonlinearity This number should be less than E-7 for germanium systems.

Determining Full Width at Half Maximum (FWHM)

FWHM is measured on the calibration spectrum during the calibration. Once the calibration is established the peaks in the subsequent spectra are judged against the calibration values The FWHM is a standardized measure of the width of the peak It typically varies directly with increasing energy

86

An increase in the size of the FWHM is a possible indication of interference from other peaks, which are very close in energy to the photopeak Depending on the resolution of the detector, peaks in the multiplets must be separated by a specified number times the FWHM to be identified as separate peaks

The FWHM is estimated by determining the maximum height of the peak (not the integral). The maximum height can usually be found at the centroid. The number of channels between the channels which represent half of the maximum height of the peak on each side of the centroid are determined. The FWHM in channels can be converted to energy once an energy calibration is established.

EFFICIENCY CALIBRATION

At this point the following is known about the peak·

    Centroid Energy
    Net Peak Area
    Collect Time

The efficiency calibration will relate the number of counts, which are found in the net peak area to the number of gamma being emitted from the source This accounts for the fact that some of the gammas emitted from the source are emitted in directions, which never reach the detector. Of those that reach the detector, many do not interact with the photoelectric interaction and thus result in pulses under the photopeak Figure A.7 shows a typical efficiency calibration curve for a Ge detector.
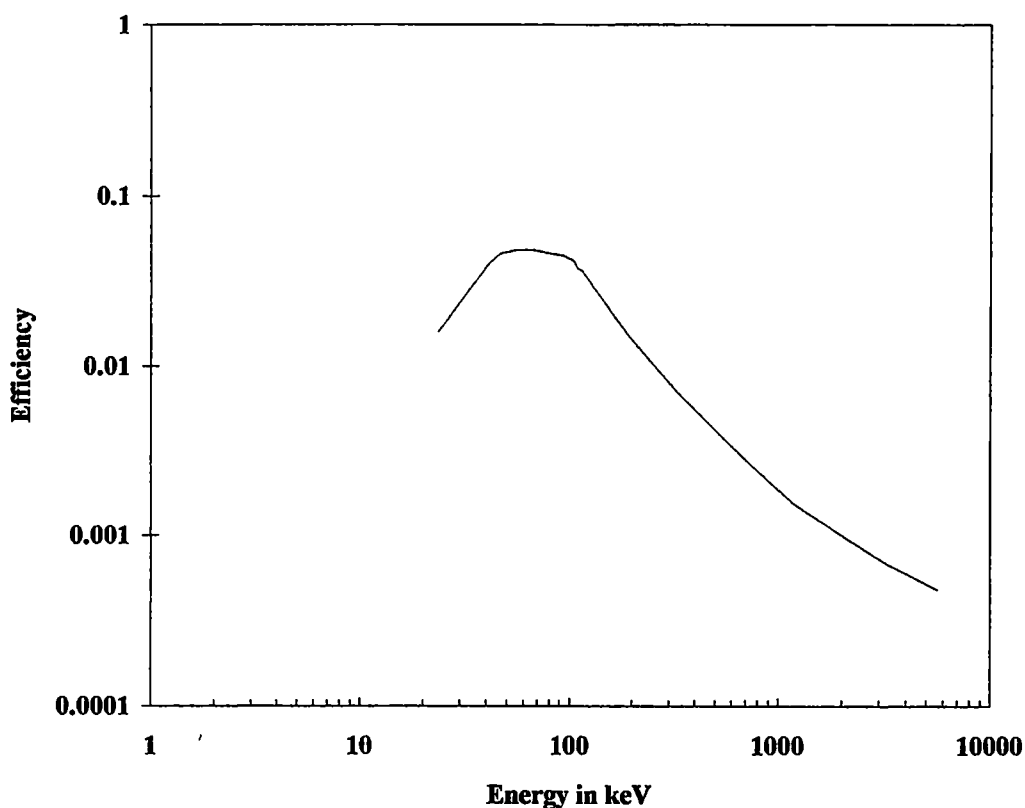
Figure A-7. Typical efficiency calibration curve

In addition to the characteristics of an energy calibration source the efficiency calibration source should

1. Be configured as closely to the expected unknowns as possible.

2 Have certified activities

3 Be collected long enough to have at least 20,000 counts in the net peak area

4 Contain peak energy at the designated crossover point

5 Be prepared so as to prevent leakage or plate-out of the contents.

6 Not create a dead time for the system significantly above that which is found with unknowns or above the limits of reliable counting.

Calculation of the Efficiency

The efficiency is calculated individually for the designated energies within the calibration

standard. The following equation is used.

$$\text{Effic}(c / \text{gamma}) = \frac{\text{Counts} / \sec}{\text{gammas} / \sec}$$

The standard must be decay corrected to the count date when manually calculating the

efficiency. The efficiency is calculated for each peak in the calibration spectrum These

are plotted on the log-log plot against the energy. The exact shape of the curve may vary

but these curves generally follow the shape shown in Figure C 7

APPENDIX B

EXPERIMENTAL DATA

BATCH EQUILIBRIUM DATA

And

EXPERIMENTAL PROCEDURE

The following tables contain the experimental data for the anion and cation batch experiments for recovery of thorium The anion ion exchange data is represented by the sample code BT The cation ion exchange data is represented by the sample code CAT. The anion flowsheet for the subsequent samples is as follows.
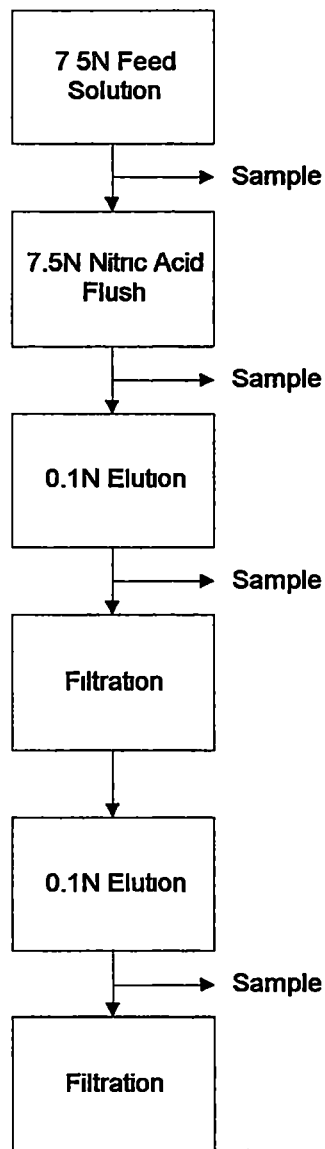
Figure B-1. Batch anion ion exchange thorium recovery flowsheet.

While, the cation flowsheet for the following samples is represented by.

```
┌─────────────────┐                        ┌─────────────────┐
│  0.1N Feed      │                        │                 │
│  Solution       │                        │   Filtration    │
│                 │                        │                 │
└────────┬────────┘                        └────────┬────────┘
         │────────────► Sample                      │
         ▼                                           ▼
┌─────────────────┐                        ┌─────────────────┐
│  0.1N Cation    │                        │  4.5M NH4Ac     │
│  Adsorption     │                        │  Elution        │
│                 │                        │                 │
└────────┬────────┘                        └────────┬────────┘
         │                                           │──────► Sample
         ▼                                           ▼
┌─────────────────┐                        ┌─────────────────┐
│                 │                        │                 │
│  1.5N Flush     │                        │   Filtration    │
│                 │                        │                 │
└────────┬────────┘                        └─────────────────┘
         │────────────► Sample
         ▼
┌─────────────────┐
│                 │
│  Filtration     │
│                 │
└────────┬────────┘
         │
         ▼
┌─────────────────┐
│  4 5M NH4Ac     │
│  Elution        │
│                 │
└────────┬────────┘
         │────────────► Sample
```
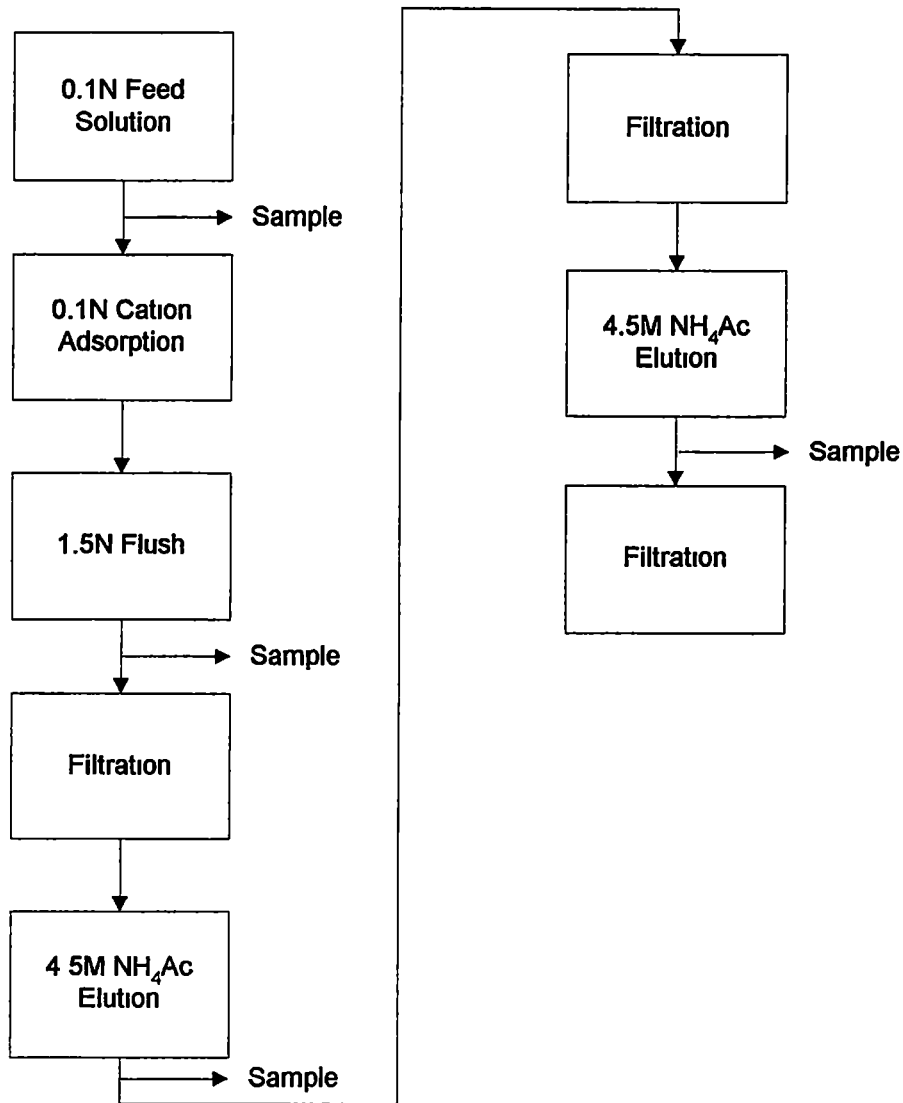
Figure B-2. Batch cation ion exchange thorium recovery flowsheet.

93

General Experimental Raschig Ring Remediation Procedure:

Equipment

- 500 ml beaker
- ultrasonic sink
- gravity filtering device
- EG&G NOMAD gamma spectroscopy unit
- stopwatch

- nitric acid or surfactant
- 0-100 °C thermometer
- scintillation vials
- 1 ml pipette
- plastic bags

Procedure

1 Take two Raschig rings contained in sealed plastic bags (e.g , sealable sandwich bags) and count the gamma activity for thorium-229 isotopes (i e., 193 keV and 210 keV) to determine the total curie activity of the sample
2 Place approximately 200 ml of solvent (i e , nitric acid or surfactant) into a 500 ml beaker.
3 Place beaker into ultrasonic sink and turn power on to ultrasonic sink.
4 Remove Raschig rings from sealed bag and place sample into beaker, while starting stopwatch
5 Using 1 ml pipe, pull 1ml samples per specified time intervals and place samples in scintillation vials
6 After completion of remediation, turn power off to ultrasonic sink and remove Raschig rings from beaker and place in sealed plastic bag
7 Perform gamma spectroscopy on 1 ml samples to determine thorium-229 concentration   The total thorium-229 concentration is determined by the product of the thorium-229 concentration per ml and the total volume (ml) of solution in the beaker at the time of the sample
8 Perform gamma spectroscopy of remediated Raschig rings to determine total activity removed

DATE	SAMPLE ID	NORMALITY	SAMPLE VOLUME(ml)	TOTAL VOLUME(ml)	Th-229 (193 KeV)	Th-229 (210 KeV)	Th-229 (avg)	TOTAL Th-229 (uCi)
4/1/96	BT-2-1	7.5 FEED	5	250	8.5584	8.7794	1 73378	433.445
	BT-2-2	7.5	5	300	0.8346	1.6534	0.2488	74.64
	BT-2-3	0 1	5	100	6.034	5 9239	1.19579	119.579
	BT-2-4	RESIN	1	100	1.7158	1.6534	1.6846	168.46
4/8/96	BT-3-1	7.5 FEED	5	250	9.6082	9.6011	1.92093	480.2325
	BT-3-2	7.5	5	300	0.8018	0.6695	0.14713	44.139
	BT-3-3	0 1	5	100	1.2197	1.085	0 23047	23.047
	BT-3-FP	FILTER	1	1	1.1959	1.7244	1.46015	1 46015
	BT-3-4	RESIN	1	100	0.3873	0.3652	0.37625	37.625
	BT-3-5	0 1 X 2	5	125	6.1937	6 1674	1.23611	154 5138
	BT-3-6	RESIN 2	1	100	0.8902	0.7557	0.82295	82.295
4/9/96	BATCH TEST 4 IN 0 1N MIX RESIN WAS DRIED COMPLETELY. BLACK IN COLOR.							
	BT-4-1	7.5 FEED	5	250	8.786	9.3525	1.81385	453 4625
	BT-4-2	7.5	5	300	1.2775	1.3339	0.26114	78.342
	BT-4-3	0 1	5	75	0.0849	0	0 00849	0.63675
	BT-4-4	RESIN	1	100	3.4009	3.4387	3 4198	341.98
4/15/96	BT-5-1	7.5 FEED	5	250	8.9946	9.392	1.83866	459.665
	BT-5-2	7.5	5	400	0.5275	0 4658	0.09933	39.732
	BT-5-3	0.1	5	200	6.275	6.0323	1.23073	246.146
	BT-5-4	RESIN		100	0.1123	0.1718	0.14205	14.205
4/18/96	BT-6-1	7.5 FEED	5	250	9.9366	9.9648	1 99014	497.535
	BT-6-2	7.5	5	400	0.7357	1.0185	0.17542	70.168
	BT-6-3	0.1	5	300	6.6211	6.7672	1 33883	401.649
	BT-6-4	RESIN	1	100	3 4475	3 5746	3.51105	351.105
	BT-6-5	FP1			0.1254	0	0.0627	0
	BT-6-6	FP2			0.2837	0 1861	0.2349	0
	BT-6-7	FP3			0.8313	0.8863	0 8588	0
4/23/96	BATCH TEST 7 STARTED WITH RESIN FROM COLUMN TEST 3							
	BT-7-1	0.1	5	100	0.2128	0.2057	0.04185	4.185
	BT-7-2	RESIN	1	100	0.0214	0.0049	0.01315	1.315

DATE	SAMPLE ID	NORMALITY	SAMPLE VOLUME(ml)	TOTAL VOLUME(ml)	Th-229 (193 KeV)	Th-229 (210 KeV)	Th-229 (avg)	TOTAL Th-229 (uCi)
4/24/96	BT-8-1	FEED 7 5	5	300	9 511	9 436	1 8947	568 41
	BT-8-2		5	400	0 6565	0 5705	0 1227	49 08
	BT-8-3	0 1	5	300	4 8776	4 7841	0 96617	289 851
	BT-8-4	RESIN	1	200	1 4031	1 5008	1 45195	290 39
	BT-8-5	0 1	5	100	7 1473	7 47	1 46173	146 173
	BT-8-6	RESIN	1	200	1 0705	1 2144	1 14245	228 49
5/1/96	BT-9-1	FEED 7 5	5	400	8 9749	9 2254	1 82003	728 012
	BT-9-2	7 5	5	400	0 5938	0 6439	0 12377	49 508
	BT-9-3	0 1	5	400	3 1802	3 2661	0 64463	257 852
	BT-9-4	RESIN	1	200	0 2243	0 1787	0 2015	40 3
5/13/96	BT-10-1	FEED 7 5	5	500	8 5758	8 7015	1 72773	863 865
	BT-10-2-1	7 5	5	5	1 0524	0 9941	0 20465	1 02326
	BT-10-2-2	7 5	5	5	1 318	1 1997	0 25177	1 25885
	BT-10-2-3	7 5	5	5	0 9963	1 1948	0 21911	1 09555
	BT-10-2-4	7 5	5	5	1 0722	0 8153	0 18875	0 94375
	BT-10-2-5	7 5	5	5	0 9254	0 7737	0 16991	0 84955
	BT-10-2-6	7 5	5	5	1 1893	1 0797	0 2269	1 1345
	BT-10-2-7	7 5	5	5	1 1035	1 2536	0 23571	1 17855
	BT-10-2-8	7 5	5	5	0 97	1 1507	0 21207	1 06035
	BT-10-2-9	7 5	5	500	0 7425	1 1581	0 19006	95 03
	BT-10-3-1	0 1	5	5	3 9473	4 0961	0 80434	4 0217
	BT-10-3-2	0 1	5	5	4 0682	4 101	0 81692	4 0846
	BT-10-3-3	0 1	5	5	3 9391	3 9027	0 78418	3 9209
	BT-10-3-4	0 1	5	5	3 9803	3 8562	0 78365	3 91825
	BT-10-3-5	0 1	5	5	3 9225	3 7044	0 76269	3 81345
	BT-10-3-6	0 1	5	5	3 5992	3 5673	0 71665	3 58325
	BT-10-3-7	0 1	5	600	3 9176	4 172	0 80896	485 376
	BT-10-4	RESIN	1	200	2 2169	2 4386	0 46555	93 11
	BT-10-5	0 1	5	400	5 0722	5 3007	1 03729	414 916
	BT-10-6	RESIN	1	200	1 5043	1 5229	0 30272	60 544
	BT-10-7	0 1	5	200	3 2606	3 5036	0 67642	135 284
	BT-10-8	RESIN	1	200	0 4239	0 4725	0 08964	17 928
5/23/96	BT-11-1	FEED 7 5	5	400	9 743	10 3738	2 01168	804 672
	BT-11-2	7 5	5	400	1 1592	1 1614	0 23206	92 824
	BT-11-3	0 1	5	200	9 3283	9 6822	1 90105	380 21
	BT-11-4	0 1X2	5	200	8 738	8 4891	1 72271	344 542

DATE	SAMPLE ID	NORMALITY	SAMPLE VOLUME(ml)	TOTAL VOLUME(ml)	Th-229 (193 KeV)	Th-229 (210 KeV)	Th-229 (avg)	TOTAL Th-229 (uCi)
5/30/96	BT-12-1	FEED	5	500	9.7253	10.7091	2.04344	1021.72
	BT-12-2	7.5	1	1	0.3013	0.3775	0.06788	0.06788
	BT-12-3	7.5	1	1	0.2694	0.1689	0.04383	0.04383
	BT-12-4	7.5	1	1	0.2322	0.0818	0.0314	0.0314
	BT-12-5	7.5	1	1	0.2304	0.0924	0.03228	0.03228
	BT-12-6	7.5	1	1	0.2552	0.33	0.05852	0.05852
	BT-12-7	7.5	1	1	0.1631	0.1452	0.03083	0.03083
	BT-12-8	7.5	1	1	0.1648	0.1557	0.03205	0.03205
	BT-12-9	7.5	1	1	0.2091	0.2006	0.04097	0.04097
	BT-12-10	7.5	1	1	0.2428	0.2244	0.04672	0.04672
	BT-12-11	7.5	1	1	0.2854	0.1161	0.04015	0.04015
	BT-12-12	7.5	1	1	0.1577	0.1927	0.03504	0.03504
	BT-12-13	7.5	1	500	0.2056	0.0871	0.02927	14.635
	BT-12-14	0.1	5	200	5.0304	4.6923	0.97227	194.454
	BT-12-15	0.1	5	200	9.9728	9.7402	1.9713	394.26
	BT-12-16	0.1	5	100	8.6688	8.6003	1.72691	172.691
	BT-12-17	RESIN	1	200	1.0848	1.0367	0.21215	42.43
6/6/96	BT-13-1	FEED	5	400	10.5764	10.4002	2.09766	839.064
	BT-13-2	7.5	5	400	1.4487	1.2755	0.27242	108.968
	BT-13-3	0.1	5	200	6.9576	6.7532	1.37108	274.216
	BT-13-4	0.1	5	200	10.4069	10.1269	2.05338	410.676
	BT-13-5	0.1	5	100	7.5253	7.4279	1.49532	149.532
6/12/96	BT-14-1	FEED	5	400	12.0701	11.8034	2.38735	954.94
	BT-14-2	7.5	5	400	2.2928	1.8378	0.41306	165.224
	BT-14-3	0.1	5	200	6.471	6.1795	1.26505	253.01
	BT-14-4	0.1	5	200	7.2895	6.945	1.42345	284.69
	BT-14-5	0.1	5	100	10.4982	9.9739	2.04721	204.721
	BT-14-6	RESIN	1	200	0.5692	0.5527	0.56095	112.19
6/25/96	BT-15-1	FEED	5	500	8.9972	8.8024	1.77996	889.98
	BT-15-2	7.5	5	500	1.5532	1.988	0.35412	177.06
	BT-15-3	0.1	5	200	6.9274	6.8046	1.3732	274.64
	BT-15-4	0.1	5	200	10.6341	10.386	2.10201	420.402
	BT-15-5	0.1	5	100	6.3817	6.4294	1.28111	128.111
	BT-15-6	RESIN	1	200	2.6171	2.5094	2.56325	512.65

DATE	SAMPLE ID	NORMALITY	SAMPLE VOLUME(ml)	TOTAL VOLUME(ml)	Th-229 (193 KeV)	Th-229 (210 KeV)	Th-229 (avg)	TOTAL Th-229 (uCi)
4/15/96	STARTED WITH ELUANT 2 FROM 3/7/96 COLUMN TEST, 200 ml VOLUME							140.19
	CAT-1-1	0.1	5	200	NONE	NONE		0
	CAT-1-2	1.5	5	300	NONE	NONE		0
	CAT-1-3	MIXTURE	5	100	6.7152	6 6413	1.33565	133.565
	CAT-1-4	MIXTURE	5	100	1.0443	1.0826	0 21269	21.269
4/22/96	STARTED WITH 0.1N FROM 3/26/96 BATCH TEST 1, 125 ml VOLUME							
	CAT-2-1	0 1	5	125	0.0791	0.0734	0.01525	1 90625
	CAT-2-2	1.5	5	300	0.0066	0.1126	0.01192	3.576
	CAT-2-3	MIXTURE	5	150	2.1377	2 0174	0.41551	62.3265
	CAT-2-4	MIXTURE	5	100	0.2045	0.377	0.05815	5.815
4/23/96	STARTED WITH 0.1N FROM 4/1/96 BT-2-3-0.1N, 100 ML VOLUME							119.579
	CAT-3-1	0 1	5	100	0.0033	0.0539	0.00572	0.572
	CAT-3-2	1 5	5	300	0	0.0049	0.00049	0.147
	CAT-3-3	MIXTURE	5	150	4.5163	4.5882	0.91045	136.5675
	CAT-3-4	MIXTURE	5	100	0.5707	0 9793	0.155	15.5
4/25/96	STARTED WITH BT-3-3(100ml) AND BT-3-5(125 ml), 225 ml VOLUME							177.52
	CAT-4-1	0.1	5	225	0	0.093	0.0093	2.0925
	CAT-4-2	1.5	5	300	0	0	0	0
	CAT-4-3	MIXTURE	5	150	7.4162	7.2961	1.47123	220.6845
	CAT-4-4	MIXTURE	5	100	1.0986	1.4054	0.2504	25 04
4/29/96	STARTED WITH 500 ml OF CELL 0.1 N SOLUTION							
	CAT-5-1	0.1	5	500	0	0.0049	0.00049	0.245
	CAT-5-2	1.5	5	300	0	0	0	0
	CAT-5-3	MIX 1	5	150	1.3971	1.5253	0.29224	43.836
	CAT-5-4	MIX 2	5	100	STOPPED TEST			
	CAT-5-5	START-0.1	5	500	0.5542	0 4799	0.10341	51.705
5/2/96	STARTED WITH 500 ML OF CELL 0.1 N SOLUTION							
	CAT-6-1	0.1	5	500	0	0.0661	0.00661	3.305
	CAT-6-2	1 5	5	300	0.0115	0	0 00115	0.345
	CAT-6-3	MIX 1	5	150	1.3443	1.2462	0.25905	38.8575
	CAT-6-4	MIX 2	5	100	0.2458	0.2252	0.0471	4.71

98

DATE	SAMPLE ID	NORMALITY	SAMPLE VOLUME(ml)	TOTAL VOLUME(ml)	Th-229 (193 KeV)	Th-229 (210 KeV)	Th-229 (avg)	TOTAL Th-229 (uCi)
5/8/96	STARTED WITH BT-5-3, BT-6-3, BT-7-1, 500 ML VOLUME							
	CAT-7-1	0.1	5	500	0.0297	0	0.00297	1.485
	CAT-7-2	1.5	5	300	0	0.0294	0.00294	0.882
	CAT-7-3	MIX 1	5	150	10.0359	10.0163	2.00522	300.783
	CAT-7-4	MIX 2	5	100	2.2463	2.064	0.43103	43.103
	CAT-7-5	START	5	500	4.866	5.1171	0.99831	499.155
5/23/96	STARTED WITH BT-8-3, BT-8-5, BT-9-3, 700 ML VOLUME							
	CAT-8-1	0.1	5	700	0	0.132	0.0132	9.24
	CAT-8-2	1.5	5	300	0.0567	0.0026	0.00593	1.779
	CAT-8-3	MIX 1	5	150	14.4931	1.3436	1.58367	237.5505
	CAT-8-4	MIX 2	5	100	4.8263	0.6282	0.54545	54.545
6/3/96	STARTED WITH CT-2-1-11, CT-3-5, CT-3-6, RESIN TEST, 400 ML VOLUME							
	CAT-9-1	0.1	5	400	0	0.0706	0.00706	2.824
	CAT-9-2	1.5	5	300	0.1143	0.0081	0.01224	3.672
	CAT-9-3	MIX 1	5	150	17.066	16.5738	3.36398	504.597
	CAT-9-4	MIX 2	5	100	4.9218	4.6353	0.95571	95.571
	CAT-9-5	START	5	400	9.1784	8.8283	1.80067	720.268
6/6/96	STARTED WITH BT-8-3, 600 ML VOLUME							
	CAT-10-1	0.1	5	600	0.0197	0.1196	0.01393	8.358
	CAT-10-2	1.5	5	300	0	0	0	0
	CAT-10-3	MIX 1	5	150	12.1749	11.9092	2.40841	361.2615
	CAT-10-4	MIX 2	5	100	1.9257	2.1922	0.41179	41.179
6/10/96	STARTED WITH BT-11-3, BT-11-4, 400 ML VOLUME							
	CAT-11-1	0.1	5	500	0.0038	0.0525	0.00563	2.815
	CAT-11-2	1.5	5	300	0.0229	0	0.00229	0.687
	CAT-11-3	MIX 1	5	150	11.1101	10.8831	2.19932	329.898
	CAT-11-4	MIX 2	5	100	0.9635	1.0861	0.20496	20.496
6/11/96	STARTED WITH BT-10-5, BT-10-7, 400 ML VOLUME							
	CAT-12-1	0.1	5	400	0.147	0.0332	0.01802	7.208
	CAT-12-2	1.5	5	300	0.0727	0	0.00727	2.181
	CAT-12-3	MIX 1	5	150	15.5121	15.2027	3.07148	460.722
	CAT-12-4	MIX 2	5	100	2.9704	2.689	0.56594	56.594
6/12/96	STARTED WITH BT-10-5, BT-10-7, 400 ML VOLUME							
	CAT-13-1	0.1	5	500	0.0956	0.0415	0.01371	6.855
	CAT-13-2	1.5	5	300	0.127	0	0.0127	3.81
	CAT-13-3	MIX 1	5	150	0	0	0	0
	CAT-13-4	MIX 2	5	100	22.5683	21.85	4.44183	444.183

Appendix C

Ultrasonic Theory

Development of a mass transfer correlation for the experimental ultrasonic system led to the discovery of a complicated mass transfer system   Experimental equipment limitations prevented an in-depth study of all the mass transfer effects that resulted from the use of ultrasonic combined with the various solvent mediums. However, a detailed development of the ultrasonic theory is presented, which provides the basis for further study and future study   A relationship is developed from the presented ultrasonic theory and dimensionless mass transfer correlations. This relationship is used to predict the effects of changing ultrasonic intensity and frequency.

The application of ultrasonic cleaning requires a fundamental review of wave theory and the effects that lead to cavitation. The particles in the ultrasonic medium commence a vibratory motion from the induced sound wave   Therefore, the particles possess kinetic energy. An energy balance on a volume element under the influence of the ultrasonic wave is shown in Figure C.1.
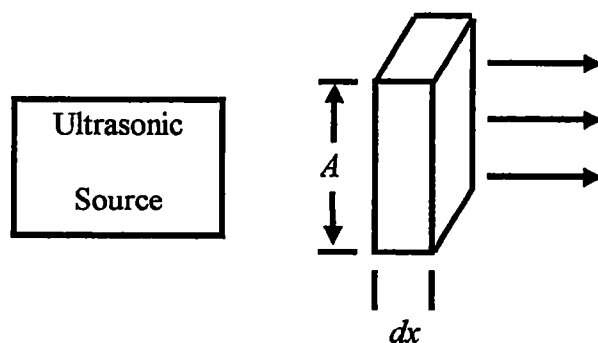

Figure C.1. Control Volume for Ultrasonic Medium

Then the kinetic energy of the volume is given by:

$$KE = \frac{1}{2}(\rho A dx)v^2 \qquad (C.1)$$

The energy of the wave E_t can be obtained by integration of Equation C.1 to yield the following.

$$E_t = \frac{1}{2}\rho A x v^2 \qquad (C.2)$$

The energy density per unit volume (i e , energy density, E) is given by

$$E = \frac{1}{2}\rho v^2 \qquad (C.3)$$

The energy density can be related to the intensity, I, by assuming that the sound energy passes through a unit area with a velocity of c,

$$I = Ec \qquad (C 4)$$

where c is the product of the frequency and the wavelength

Then from Equation C 3, the intensity is defined by,

$$I = \frac{1}{2}\rho c v^2 \qquad\qquad\qquad \text{(C 5)}$$

The application of the acoustic wave pressure, P_a, will cause the particles suspended in the medium to be displaced in the direction of the wave. For a given finite element, the sound wave with a velocity c will pass a distance in dx/c seconds. Therefore, the acceleration of the particles in this volume element will be approximately vc/dx (velocity/time) Consequently, the relationship of the force applied to the particles in the same element can be derived from the acoustic wave pressure

$$\frac{P_a}{v} = \rho c \qquad\qquad\qquad \text{(C 6)}$$

For maximum particle velocity, v_o, the amplitude of the oscillating acoustic pressure, P_A is given by the expression

$$\frac{P_A}{v_o} = \rho c \qquad\qquad\qquad \text{(C 7)}$$

or

$$v_o = \frac{P_A}{\rho c} \qquad\qquad\qquad \text{(C 8)}$$

Thus, the intensity of the sound wave from Equations C.5 and C 8 is proportional to the square of the acoustic amplitude

$$I = \frac{P_A^2}{2\rho c} \qquad \text{(C 9)}$$

The relation for the intensity, I, at some distance, d, from the source is expressed by

$$I = I_o \, exp(-2\alpha d) \qquad \text{(C.10)}$$

where α is the absorption (attenuation) coefficient. Attenuation is the consequence of reflection, refraction, diffraction, or mechanical conversion to heat. According to Stokes, the absorption coefficient in a liquid as a result of frictional losses, α_s, is given by

$$\alpha_s = 8\eta_s \pi^2 f^2 / 3\rho c^3 \qquad \text{(C 11)}$$

where η_s is the ordinary (or shear) viscosity of the liquid [34]

Kirchoff has suggested that energy losses due to heat (thermal) conduction in the medium must also be considered During instances of high pressure, temperatures will be elevated above mean temperature, while during low pressure, temperatures will be below the mean temperature [35]. This results in a sound absorption coefficient given by:

104

$$\alpha_{th} = 2\pi^2 K \frac{(\gamma - 1)f^2}{(\rho \gamma C_v c^3)}$$ (C 12)

The absorption as a result of viscosity and thermal conductivity is referred to as classical absorption, α_{cl}, and is given by

$$\alpha_{cl} = \alpha_s + \alpha_{th} = \frac{2\pi^2}{\rho c^3} \left\{ \frac{4}{3}\eta_s + \frac{(\gamma - 1)K}{\gamma c_v} \right\}$$ (C.13)

where $C_p/C_v = \gamma$

The effect of the compressional viscous forces, which act during compression and rarefaction, is associated with the bulk viscosity, η_B Equation C 13 then becomes the following.

$$\alpha = \frac{2\pi^2 f^2}{\rho c^3} \left\{ \frac{4}{3}\eta_s + \eta_B + \frac{(\gamma - 1)K}{C_p} \right\}$$ (C.14)

The bulk viscosity, η_B, in Equation C 14 refers to viscosity effects that are a result of energy losses associated with the flow of liquid molecules between positions of different densities and the relaxation processes. Overall, the effect of viscosity on the medium results in an increase in the acoustic pressure required to induce cavitation

The subsequent relationship is the determination of the critical pressure, P_K, to the bubble radius, R_e For a bubble in a given medium to remain in equilibrium, the forces that act on the bubble walls must be equivalent For the case of expansion, the bubble pressure, P_{bub}, will be a result of the sum of the trapped gas and vapor pressure in the bubble, such that·

$$P_{bub} = P_v + P_g$$ (C 15)

For the case of contraction the pressure, P_L, is the combined effect of the hydrostatic pressure, P_h, of the medium and the surface tension effect given by.

$$P_L = P_h + \frac{2\sigma}{R_e}$$ (C 16)

At equilibrium, the pressure associated with the liquid, P_L, equals the internal pressure of the bubble, P_{bub}.

$$P_h + \frac{2\sigma}{R_e} = P_v + P_g$$ (C.17)

A change in the hydrostatic pressure, $P_h' = P_h + \Delta P_h$, will result in a differential change, dR, in the equilibrium radius, R_e, to a new bubble radius R With a simplified

assumption of ideal gas behavior, the new gas pressure, $P_g' = P_g + \Delta P_g$, inside the bubble

is a ratio of the radii and the new bubble pressure, P_{bub}', and is given by

$$P_{bub}' = P_v + P_g' = P_v + P_g \left(\frac{R_e}{R} \right)^3 \qquad \text{(C.18)}$$

Expansion of the bubble will decrease the surface tension effects. Therefore, the effect of

this decreased surface tension on the new liquid pressure, P_L', is given by

$$P_L' = P_h' + \frac{2\sigma}{R} \qquad \text{(C.19)}$$

If the bubble is to maintain equilibrium then $P_L' = P_{bub}'$

$$P_h' + \frac{2\sigma}{R} = P_v + P_g' = P_v + P_g \left(\frac{R_e}{R} \right)^3 \qquad \text{(C 20)}$$

This equilibrium establishes the cubic dependence of the bubble radius on the

hydrostatic pressure of the medium, P_h' The critical hydrostatic pressure is achieved

when a small change in the pressure causes a dramatic increase in R. In other words, the

bubble becomes unstable and explodes (i e , cavitation)   The radius at which this occurs

can be termed the critical radius, R_K, and can be found when dP_h'/dR is practically zero

This can be estimated by differentiating Equation C.20 and equating to zero.

$$0 = -3P_g \frac{R_e^3}{R^4} + \frac{2\sigma}{R^2} \qquad (C\ 21)$$

At the critical radius, $R_K = R$, and substitution yields

$$R_k^2 = \frac{3}{2\sigma} P_g R_e^3 \qquad (C\ 22)$$

Also, at the critical radius, the critical pressure can be denoted as P_K, and substituted into Equation C.20.

$$P_K = P_v + P_g \left(\frac{R_e}{R_K}\right)^3 - \frac{2\sigma}{R} \qquad (C\ 23)$$

Follow on substitution of Equation C.22 into Equation C.23 yields

$$P_K = P_v - \frac{2}{3} \left\{ \frac{(2\sigma/R_e)^3}{P_g} \right\}^{0.5} \qquad (C.24)$$

108

Finally, substitution of Equation C.17 for P_g and the assumption of negligible effect from vapor pressure yields;

$$P_K = -\frac{2}{3}\left\{\frac{(2\sigma/R_e)^3}{3(P_h + 2\sigma/R_e)}\right\}^{0.5}$$

(C.25)

From Equation C.25 it is evident that a negative pressure must be applied to generate a bubble of radius R_e. With the assumption that the hydrostatic pressure is the primary resistance to the formation of cavitation bubbles, the critical pressure can be related to the quantity known as the Blake threshold pressure, P_B [36]. For relatively large bubbles where $2\sigma/R_e \ll P_h$, the Blake threshold pressure, P_B, is approximately equivalent to the hydrostatic pressure, P_h,

$$P_B \approx P_h + \frac{8\sigma}{9}\left\{\frac{3\sigma}{2P_hR_e^3}\right\}^{0.5}$$

(C.26)

and for small bubbles where $2\sigma/R_e \gg P_h$,

$$P_B \approx P_h + \frac{0.77\sigma}{R_e}$$

(C 27)

The effect of temperature is directly related to the induced effect the temperature change has on the surface tension (σ) or viscosity (η) of the medium [37] For pure compounds, the effect of temperature on surface tension is given by Jasper [38].

$$\sigma = a - bT \qquad\qquad (C.28)$$

where a and b are empirical constants

However, the mediums used in the ultrasonic cleaning method become contaminated with the particles that are removed from the components subject to cleaning This leads to more complicated mathematical estimates for the surface tension and error in the Jasper equation Still, the common effect of increasing temperature is to decrease the surface tension

In addition, the effect of increasing temperature on a liquid is usually to decrease the viscosity. A detailed discussion of various methods of predicting viscosities is found in The Properties of Gases & Liquids [39]. A common equation for estimation of liquid viscosity from the freezing point to the normal boiling temperature is given by

$$ln\,\eta_L = A + \frac{B}{T} \qquad\qquad (C.29)$$

where A and B are empirically determined parameters

The intensity, amount of energy per unit area, of the ultrasonic wave in the medium has a significant effect on the overall bubble formation However, for the experiments performed to determine the remediation effectiveness of various mediums and temperatures on the Raschig rings, the source intensity was held at a constant frequency of ~55 kHz.

Application of a mass balance across a stationary volume element proves a very difficult equation to solve (Fig C.2). However, derivation of the equation does provide insight as to the potential effect of the induced cavitation rendered by the ultrasonics.
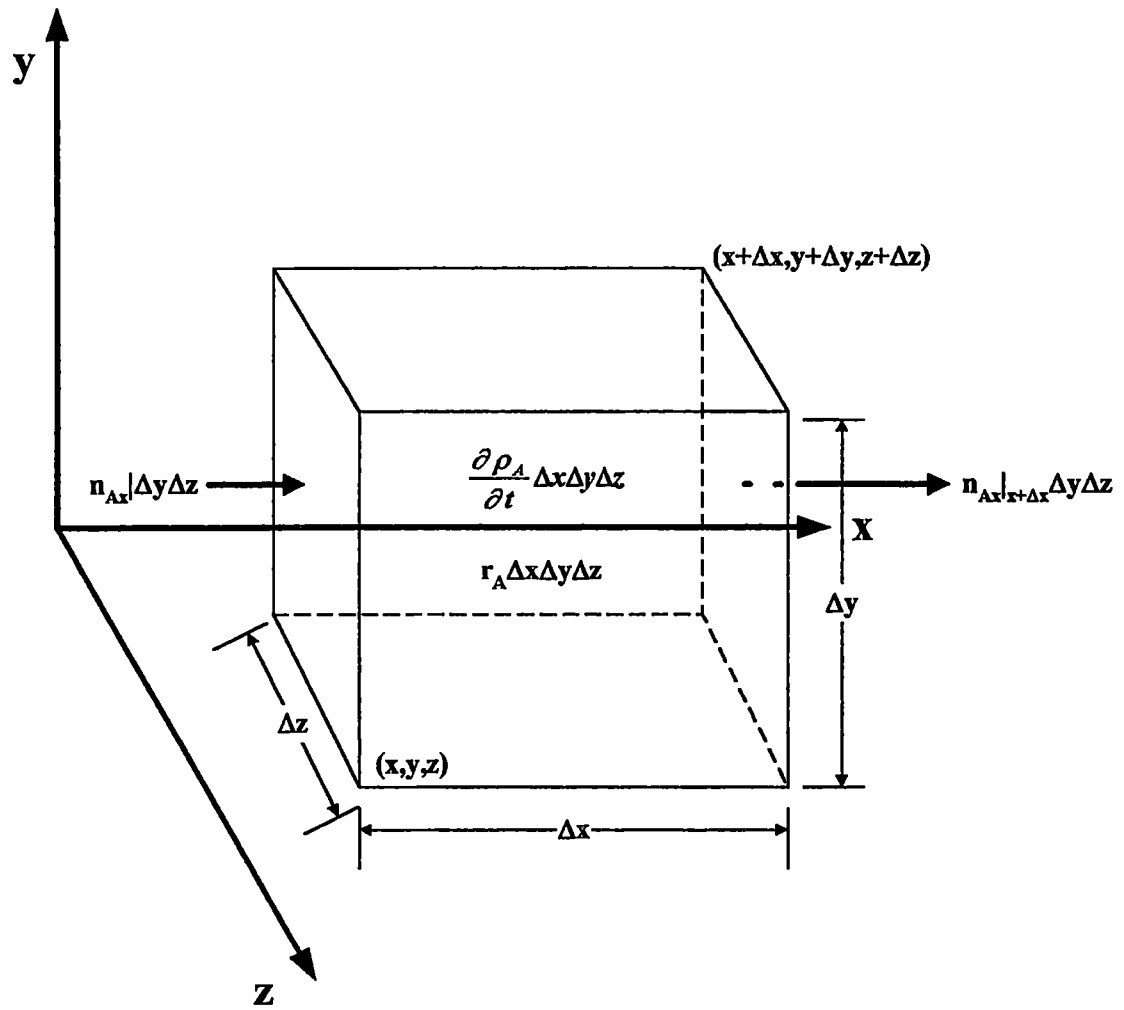
Figure C.2 Control Volume for Species Balance

The contributions to the mass balance are.

time rate of change of mass A in the volume element	$\dfrac{\partial \rho_A}{\partial t} \Delta x \Delta y \Delta z$	(C.30)
input of species A across face x	$n_{Ax}\big|_x \Delta y \Delta z$	(C.31)
output of species A across x + Δx	$n_{Ax}\big|_{x+\Delta x} \Delta y \Delta z$	(C 32)
rate of production of species A by chemical reaction	$r_A \Delta x \Delta y \Delta z$	(C 33)

The complete Cartesian coordinate mass balance accounts for the mass transport in the -x and -y directions. When the full mass balance is divided through by Δx Δy Δz and the limit is taken as Δx Δy Δz $\rightarrow$ 0 the following partial differential equation is obtained

$$\frac{\partial \rho_A}{\partial t} + \frac{\partial n_{Ax}}{\partial x} + \frac{\partial n_{Ay}}{\partial y} + \frac{\partial n_{Az}}{\partial z} = r_A \qquad (C.34)$$

With the convective mass transfer assumed to be the primary method of mass transport in the ultrasonic remediation experiments The continuity equation can be given by [40]·

$$\frac{\partial \rho}{\partial t} = -\left(\frac{\partial}{\partial x}\rho U_x + \frac{\partial}{\partial y}\rho U_y + \frac{\partial}{\partial z}\rho U_z\right) \qquad (C.35)$$

which is obtained similarly as the mass transfer Equation C.34 and must be coupled with the mass transfer equation to define the physical environment of the ultrasonic medium.

The complex boundary conditions as a result of the cavitation make explicit solutions to Equations C.34 and C.35 very difficult. This is partially a result of unstable bubble formation at the surface, external to the surface, and under the surface of the contaminants (Fig. C.3) [41, 42].
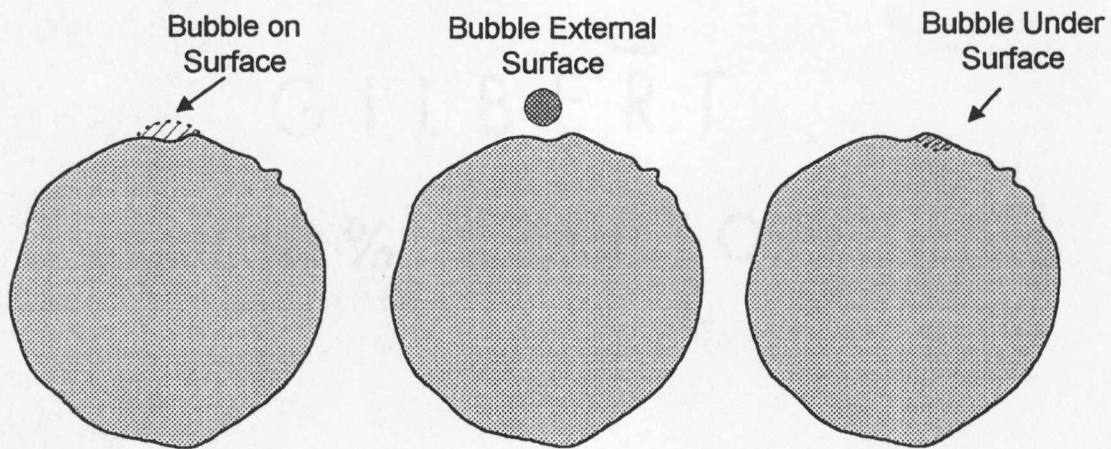

Figure C.3 Bubble Formation from Ultrasonically induced Cavitation

Typically, dimensional analysis would be used to nondimesionalize the set of transport equations and determine which dimensionless groups control the behavior of the

solutions. From this approach the design for experimental investigation could be performed on the system of interest. However, this was outside the primary objective of the project and an approximation of the mass transport is made from other physical systems that are similar in nature

Qi and Brereton [43] have performed detailed derivation of contaminant removal for ultrasonic systems where the critical pressure has not been achieved. For this case, the modes of force are the plane and focused wave fields induced by the ultrasonic source. Therefore, the evaluation of contaminant removal is one where the force of the induced ultrasonic wave must overcome the adsorption properties of the contaminants. This leads to a correlation of the intensity of the ultrasonic wave to the adhesion forces

Following this logic, a mass transfer coefficient and associated nondimensional numbers that model the ultrasonic system with cavitation could be derived as a relation to the intensity, I, of the induced ultrasonic field Obviously, this physical system is too complicated to be fully defined by any simplistic model. However, significant work has been performed on turbulent systems with eddies in the turbulent flow region. This concept of eddies and turbulent flow is applied to the ultrasonic remediation system as potentially the most applicable model available

The typical diffusion coefficient for turbulent mass transfer is the eddy diffusion coefficient, E_D, which is given by

$$E_D = -\frac{n_A}{\partial C_A / \partial y} \qquad (C.36)$$

115

where,

n_A　=　Molal flux, gmoles/s·cm^2,

C_A　=　Concentration of species A, gmoles/cm^3,

y　=　Space coordinate, cm.

The total diffusion is the sum of the molecular diffusion coefficient and the eddy diffusion coefficient However, the insignificant contribution of the molecular diffusion coefficient is neglected. Typical mass transfer theories, such as Penetration and Surface Renewal, apply an expression for the mean-square displacement of the particles, after a defined time interval, from an initial position. However, the random nature of the cavitation caused by the ultrasonics creates a turbulent flow region which could be similar to the eddys produced at the turbulent boundary area associated with the simple mass transfer models

For a turbulent flow system, an eddy viscosity, E_v, would be defined as a ratio of the shear stress to the mass velocity gradient in the turbulent region For a Newtonian fluid, the eddy viscosity can be defined by [28].

$$E_v = -\left(\frac{\tau}{d(\rho U)/dy} + k_V \right) \qquad (C.37)$$

where,

τ = Shear stress, g/cm^2,

ρ = Density, g/cm^2,

U = Time mean velocity in x direction, cm/s,

y = Space coordinate, cm,

k_V = Kinematic viscosity, cm^2/s

Typically, turbulent motion is described in terms of its intensity, which relates the magnitude of the velocity fluctuations and some defined scale or magnitude of the flow fluctuations However, for the ultrasonic cavitation system, the turbulent motion is described in terms of the intensity of the induced ultrasonic wave. From Equation C.4, the intensity is defined by the energy density, E, and the induced sound velocity, c. Where c is given by

$$c = \lambda f \qquad (C\ 38)$$

where,

λ = Wavelength, cm,

f = Frequency, s^{-1}

117

The relationship of c to the acoustic pressure, P_a, and the critical pressure, P_K, has been associated with the conditions required for cavitation Therefore, the standard time mean velocity, U, for turbulent flow is replaced with the induced sound velocity, c.

Likewise, the kinematic viscosity, v, must account for the changes in viscosity as a result of the ultrasonic wave This was defined in Equation C.14 as the bulk viscosity, η_B A bulk kinematic viscosity is defined by.

$$v_B = \frac{\eta_B}{\rho} \tag{C.39}$$

A mean kinematic viscosity, $\overline{k_M}$, is the weighted average of the bulk kinematic viscosity, k_B, and the kinematic viscosity, k

The relationships for induced ultrasonic sound velocity, c, and the mean kinematic viscosity, $\overline{k_M}$, are substituted into Equation C 36 to define a new ultrasonic eddy viscosity, E_{Uv}

$$E_{Uv} = -\left(\frac{\tau}{d(\rho c)/dy} + \overline{k_M} \right) \tag{C 40}$$

From the eddy diffusivity and ultrasonic eddy viscosity, a turbulent dimensionless number that provides a ratio of the diffusivity of momentum to the diffusivity of is the turbulent Schmidt number as presented in Section 4 1

118

Appendix D

FORMULAS AND ESTIMATES FOR ECONOMIC ANALYSIS

The following formulas were used to evaluate the cost comparisons for the nitric acid/ultrasonic system and surfactant/ultrasonic system

$$S = P\frac{e^{rn} - 1}{r} \qquad \text{(D 1)}$$

where,

S = discrete lump-sum payments as future worth,

P = present principal (or present worth),

r = inflation rate percentage, and

n = number of years money is invested.

Future value of capital investment costs were evaluated with the following formula·

$$FV = Pe^{rn} \qquad \text{(D.2)}$$

where,

FV = future value costs,

P = present worth,

r = inflation rate percentage, and

n = number of years money is invested.

Capitalization costs were estimated with the following formula.

$$\text{Capitalized cost} = C_v + \frac{C_R}{(1+i)^n - 1} \tag{D.3}$$

where,

C_v = Original cost of equipment

C_R = Cost for replacement of the equipment at end of useful life.

i = interest rate

Estimates for labor costs for operations were based on the following standards.

Labor Classification	Base Rate ($)	Burdened Rate ($)
Operator	20 00	40.00
Radiological Control Technician	19 00	38.00
Health and Safety	30.00	60 00
Superintendent	30 00	60.00
Operations Manager	45 00	90.00

Appendix E

Determination of Minimum Mass of Ion Exchange Resin

Determination of Minimum Mass of Ion Exchange Resin

The mass of ion exchange resin is determined on a dry equivalent basis. The mass of resin, for 100%, loading on a dry weight basis for complete adsorption for species A, where for this experimental species A was Th^{+n} or, $Th(NO_3)_n^{4-n}$, was determined by [44]

$$M_R = \frac{N_A}{DWC}$$

(E.1)

where,

M_R $=$ mass of resin, grams

N_A $=$ normality of species A, eq/liter

DWC $=$ dry weight capacity of resin, eq/kg dry resin

VITAE

Kenneth Givens was born in Russellville, Kentucky He attended Warren Central High School in Bowling Green, Kentucky where he graduated in 1983. Kenneth immediately joined the United States Navy and served in the Naval Nuclear Power Program. Kenneth received numerous commendations and medals for outstanding performance while serving his country in the Middle East and Mediterranean Upon honorable discharge from the United States Navy in 1989, Kenneth proceeded to pursue an undergraduate degree in Chemical Engineering from the University of California San Diego. Here, Kenneth graduated with a Bachelor in Science in Chemical Engineering in 1993. Kenneth proceeded to attain employment at Oak Ridge National Laboratory with the Chemical Technology Division While at the Oak Ridge National Laboratory, Kenneth obtained funding to pursue this thesis and additional work in the field of radioactive remediation and medical radioisotopes through the Oak Ridge National Laboratory Director's Research and Development Program In 1995 at the Ninth Symposium on Separation Science and Technology for Energy Applications, Kenneth presented a poster presentation on the "Remediation of Borosilicate Raschig Rings," which led to publication in Separation Science and Technology. In 1998, Kenneth received his Professional Engineering License for the State of Tennessee